

# Channel-Aware Latency Tail Taming in Industrial IoT

Qihao Li<sup>1</sup>, Member, IEEE, Jiayin Chen<sup>2</sup>, Member, IEEE, Michael Cheffena<sup>3</sup>, and Xuemin Shen<sup>4</sup>, Fellow, IEEE

**Abstract**—In this paper, we propose a novel channel-aware latency taming scheme, called **Optimal Transmission Latency Taming (OTLT)**, to detect hidden channel state and tame the distribution tail of the packet sojourn time in Industrial Internet of Things (IIoT) devices. Specifically, we design a forward algorithm based on a hidden semi-Markov model to detect the hidden channel state, with a particular emphasis on the state sojourn duration, and to calculate the corresponding channel access probability. Then we develop a time-sensitive model to investigate the minimum sojourn time a packet spends in the IIoT device before leaving successfully. With the obtained channel access probability, the first passage probability of the proposed model is explored to find the maximum probability of a packet being successfully transmitted in a given back-off sojourn duration (BSD). The distribution tail of the packet sojourn time can be tamed by minimizing the cumulative summation of each BSD in consideration of the quadratic penalty latency constraints. Simulation results demonstrate that, in the industrial environment, the OTLT scheme can keep the packet's sojourn duration within a quantifiable limit and variance. It can also obtain considerably efficient control over packet transmission latency in a time-varying wireless propagation channel even with the increasing number of IIoT devices.

**Index Terms**—Industrial IoT, latency taming, hidden semi-Markov model, first passage probability.

## I. INTRODUCTION

RECENT advance in wireless communications and computation have extended the Internet of Things from home and working environments to the industrial domain [1], [2], [3]. To enable automation applications in Industrial Internet of

Things (IIoT), numerous devices (sensors) have been deployed to collect and transmit data in real-time for the operation optimization and strategic decision-making [4], [5], [6]. However, to ensure quality control throughout the production process, packet transmission must fulfill stringent latency requirements of specific industrial applications [7]. Transmission protocol design based on conventional average latency is insufficient to meet the stringent latency requirements since average latency often ignores the occurrence of extreme high latency events [8]. A transient latency spike can be identified by the sharp rise of the latency distribution tail, which results in an increase in transmission latency and a detrimental influence on overall performance [9]. Hence, controlling the tail of the latency distribution is of paramount importance to meet extremely low latency requirements and keep latency within a quantifiable variance for industrial manufacturing.

In IIoT networks with a star topology, the packet transmission latency can be separated into a deterministic component and a random component [10], [11], [12]. The deterministic component specifies the minimum latency, and random components influence the latency distribution and, in particular, its distribution tail [13]. In this paper we focus on the random component, i.e., the packet sojourn time, which refers to the total amount of time a packet spends in the device waiting for an idle channel and, if required, attempting retransmission until the packet is successfully transmitted. Medium access control (MAC) protocols (e.g., IEEE 802.15.4 protocol) play an important role in limiting packet sojourn time by coordinating channel detection and managing packet transmission. In the protocol, a transmission cycle consists of packet back-off sojourn duration (BSD), carrier sensing access (CCA) processing delay, data transmission delay and ACK transmission delay, among which only BSD is the random component. We define the BSD as the time duration in which a packet waits for channel detection in a transmission cycle. The packet sojourn time is the cumulative summation of all the BSDs of this packet until being transmitted successfully.

However, it is challenging to shorten the distribution tail so as to control the random component of packet transmission latency in the harsh industrial environment. First, IIoT devices cannot accurately determine the channel state, with a particular emphasis on the state sojourn duration, and properly integrate the corresponding channel access probability into the BSD control strategy. In the industrial environment, the channel can be contaminated by impulse noise and interference effects, which change the channel states over time between a finite set, with the changing occurring at unknown periods in time [14].

Manuscript received 7 February 2022; revised 28 June 2022 and 4 November 2022; accepted 12 January 2023. Date of publication 30 January 2023; date of current version 12 September 2023. This work was supported in part by the National Natural Science Foundation of China under Grant 62201148, in part by the Guangdong Province Basic and Applied Basic Research Foundation under Grant 2022KQNCX, in part by the Key Area Research and Development Program of Guangdong Province under Grant 2020B0101110003, and in part by the Research Grant from the Regional Research Fund of Norway (RFF). The associate editor coordinating the review of this article and approving it for publication was L. Giupponi. (Corresponding author: Qihao Li.)

Qihao Li is with the School of Electrical Engineering and Intelligentization, Dongguan University of Technology, Dongguan, Guangdong 523000, China (e-mail: qihao.li@ieee.org).

Jiayin Chen is with the Department of Electrical and Computer Engineering, University of British Columbia, Vancouver, BC V6T 1Z4, Canada (e-mail: jiayinchen@ece.ubc.ca).

Michael Cheffena is with the Faculty of Engineering, Norwegian University of Science and Technology, 2815 Gjøvik, Norway (e-mail: michael.cheffena@ntnu.no).

Xuemin Shen is with the Department of Electrical and Computer Engineering, University of Waterloo, Waterloo, ON N2L 3G1, Canada (e-mail: sshen@uwaterloo.ca).

Color versions of one or more figures in this article are available at <https://doi.org/10.1109/TWC.2023.3239531>.

Digital Object Identifier 10.1109/TWC.2023.3239531

1536-1276 © 2023 IEEE. Personal use is permitted, but republication/redistribution requires IEEE permission.

See <https://www.ieee.org/publications/rights/index.html> for more information.

Each occurrence of a particular state has a random sojourn duration, which can be modelled as a random variable according to a probability distribution associated with that state. The channel state sojourn duration is rarely taken into account in the conventional channel detection schemes. In addition, the channel impairments can distort the transmission signal, causing the channel to be interfered in a set of time slots grouped in bursts [15]. Thus, the statistics of the fading process may be non-stationary over a period of time. It means there can be a channel state hidden behind the detected results, which leads a device to mistake a “Busy” channel for an “Idle” one. As a result, packets will crowd into the network, create more collisions, affect the packet BSD control decision, perturb the packet sojourn time’s standard deviation and finally result in long tail of latency distribution in each device.

Second, it is difficult to regulate the timing bounds of the packet sojourn time distribution, in particular the distribution tail, because the packet sojourn time inherits a heavy-tailed distribution from collision and channel access failure [16]. In the conventional MAC schemes, the current BSD is decided only on the basis of the present system state instead of historical BSD results [17]. That means there is no quantified limitation on controlling the distribution tail of the packet sojourn time. But according to the collision avoidance defined in 3GPP Release 15, the packet BSD is determined by generating random numbers from uniform distribution over a pre-designed time slot [18], [19]. The BSD should be generated based on previous BSD results, which results in an impact on the aggregate total BSD load. Therefore, to analyze the packet sojourn time and model its distribution tail, a new time-sensitive model (TSM) should be built, which considers the memory property, channel access probability and the packet BSD in each transmission cycle.

Third, the delay-insensitive back-off control strategy based on examining BSD average values is unable to tame the distribution tail of the packet sojourn time, because latency variance and extreme high latency events are always neglected when evaluating only average [8]. Because of this tail, the average value becomes larger than the distribution’s most probable value. The fluctuation around the maximum of this distribution becomes greater. If we still design the control strategy based on the average value, the generated BSD results will lead to a negative impact on overall performance [20]. Thus, to maintain the packet sojourn time within the timing limitations, the BSD must be fine-grainedly updated through computing the optimal BSD in the direction of the control gradient, which can lead to the minimum packet sojourn time. These challenges motivate our design to fulfill the latency requirement in IIoT.

In this paper, we focus on how to detect the hidden channel state considering the industrial noise and interference effects, and minimize the distribution tail of the packet transmission latency. We propose a channel-aware latency taming scheme, called Optimal Transmission Latency Taming (OTLT), to estimate the channel condition and tame the latency distribution tail through controlling the packet BSD. Specifically, the OTLT scheme is built on a channel detection module and a packet BSD control module. In the channel detection module,

we build a hidden semi-Markov model (HSMM) to characterize the industrial channel properties and a forward algorithm to detect the hidden channel state. Considering obtained channel detection result and corresponding channel access probability, in the packet BSD control module, we utilize semi-Markov model to develop a TSM to analyze the distribution tail of the packet sojourn time and calculate the optimal packet BSD to tame the tail of packet sojourn time. The following are the paper’s primary contributions.

- We investigate the channel fading duration and consider it as the sojourn duration of each hidden state in the proposed HSMM. All the related parameters in the HSMM are iteratively updated by a proposed Expectation Maximization (EM) algorithm in the result that the channel detection accuracy can be improved.
- We develop a TSM to describe the distribution tail of the packet sojourn time and build the relation between the packet BSD and the historical BSD decisions to solve the BSD memoryless shortage. In particular, we inventively find that the extreme value probability which can be used to characterize the latency tail probability is closely related to the first passage time probability of the proposed time-sensitive model. We evaluate the first passage probability (FPP) by calculating the probability of the first passage time (FPT) that a packet transfers from one system state to the state that indicates the successful delivery of the packet for the first time in a given packet BSD. Then, we investigate the FPP to find the best timing to transmit the packet with a proper packet BSD. We find that, in each transmission cycle, there is always an optimal packet BSD corresponding to the maximum FPP.
- We investigate the average packet sojourn time by accumulating all the historical BSD with corresponding FPP and calculate the optimal BSD by minimizing the sojourn time in consideration of quadratic penalty latency constraints. The optimum packet BSD is found by iteratively investigating the optimal control scale in the direction of the control gradient, which can minimize the packet sojourn time and shorten the latency distribution tail.

The remainder of this paper is organized as follows. The related works are discussed in Section II. Section III describes the system model, and Section IV presents the problem formulation. In Section V, we discuss the proposed OTLT scheme. Simulation results are presented in Section VI to evaluate the proposed solution. Finally, in Section VII, we conclude this research work.

## II. RELATED WORK

Various schemes have been investigated for detecting channel state, analyzing the performance and applicability of collision avoidance schemes, as well as controlling the packet transmission latency in a delay constrained network. A proposed latency control scheme in optimizing the packet transmission delay consists of a channel detection phase and a BSD control phase. In the channel detection phase, the device measures the channel quality to verify whether the channel is

idle. If the channel is busy, the BSD control phase is then used to avoid packet collisions through delaying the transmission for a time period.

The channel state detection plays a critical role in decreasing the packet collision ratio and improving the efficiency of wireless resource utilization. Bhowmick et al. designed a channel estimation scheme for predicting future channel state based on historical channel estimation results in order to enhance the channel access efficiency [21]. Given a set of historical channel observations, Eltom et al. modeled the channel state into a hidden Markov model (HMM) and proposed a scheme to predict the channel state by recursively calculating the posterior probability of the HMM [22]. However, little attention is paid to build a channel detection scheme for devices in an industrial environment, where the wireless channel state is time-varying due to the multipath fading and interference effects. These fading dips can reverse the channel state by dropping considerably below the proper threshold in a short period. In addition, the average duration of the channel state and the latent parameters of the related proposed model are rarely jointly taken into account.

Apart from the channel detection phase, when the channel state is busy, the BSD control phase is utilized to avoid packet collision. A plenty of BSD resolution approaches have been proposed for reducing the number of packet collision and minimizing the packet transmission delay. The studies on deterministic backoff [23] and centralized random back-off [24] indicate that the collision probability can approach zero. Deterministic backoff scheme prepares a collision-free timetable in a fully decentralized way with a predetermined backoff stage for each devices after successfully accessing the channel [23]. By contrast, centralized random backoff scheme schedules the packet transmission using an acknowledgment packet that specifies the backoff stage generated by a virtual backoff algorithm running in the access-point [24]. Gomes et al. designed a smart guaranteed time slot allocation scheme to improve the utilization of the contention free period in a super-frame which starts with a beacon frame sent by the coordinator [25]. By employing these active periods, the average transmission latency for message delivery among devices (e.g., sensors) is supposed to meet the industrial application requirements.

However, due to the impact of the interference effects in the industrial environment, the devices can miss their assigned transmission slot and aggravate the long-tailed features of the transmission latency. When the device with time-critical traffic continues to detect a busy channel state and contends with other devices in remaining time slots, it will be difficult for devices demanding time-critical service to transmit packets on time. In an industrial environment with a large number of devices, the existing works show that the collision probability decreases as the minimum backoff window size grows [7]. But, when the backoff window size grows, the channel idle time, i.e., vacant time slots, grows as well. The enormous delay time will result in the increment of high latency events, which expands the latency distribution tail and increases the packet deadline miss ratio. Liu et al. characterizes the tail of the latency distribution using the extreme value theory to measure

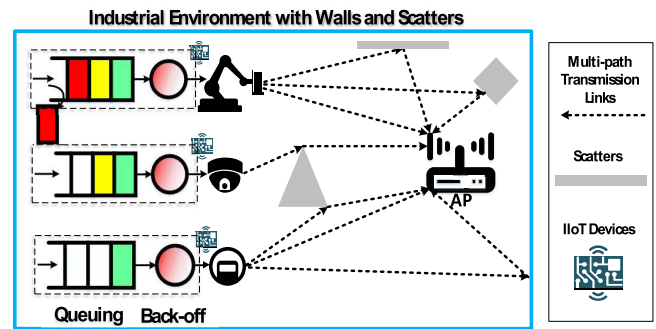


Fig. 1. Network model.

the delay behavior of the sensor devices in the industrial IoT networks [26]. But very few of works study the impact of the historical BSD results latency on the distribution tail with the consideration of channel state in an industrial environment.

All the aforementioned works provide interesting results but pay little attention to the joint investigation of the channel detection methods and the impact of the channel detection results on generating the packet BSD in the industrial environment. Questions remain open regarding characterizing the distribution of packet sojourn time and taming the distribution tail of the packet sojourn time by iteratively controlling the packet BSD in each transmission cycle. In this paper, our target is to detect the channel state hidden in the noisy channel and tame the distribution tail of the packet sojourn time within a stringent bound.

### III. SYSTEM MODEL

#### A. Network Model

As shown in Fig. 1, two types of components make up the entire network: one access point (AP) and several IIoT devices. The network is built using a star topology, in which all devices connect with the central AP. There are many scatters uniformly distributed in the environment. The transmitted signal from devices is vulnerable to heavy multipath fading effects caused by reflections from these scatters. In this star network, a large amount of packets are transmitted from the devices to the AP. There is only one active device occupying the medium after successfully accessing the channel. All the other devices have to wait and keep their data packets in their transmitting buffer until an idle channel state is detected. IEEE 802.15.4 standard governs the AP-device association mechanisms and the medium access strategies [17].

#### B. Channel State Detection Model

When a device sends data packets to an AP, all other devices within this device's coverage continuously detect the channel to check the channel state i.e., idle or busy state for packet transmission. Since the channel state is recurrent, when the devices and AP are in a similar industrial environment, revisiting the same channel state may return almost same channel detection results. Thus, we design an HSMM to build the process of transitioning among different hidden channel states in accordance with their sojourn durations in order to

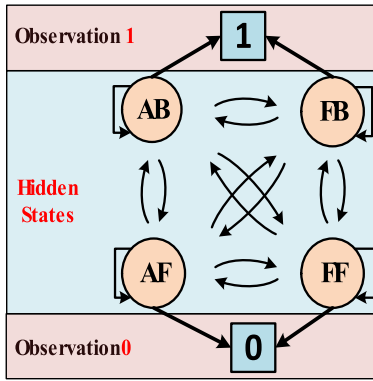


Fig. 2. Hidden semi-Markov model.

estimate the hidden channel state and calculate the appropriate channel access probability.

Let  $\mathbb{N}_+ = 1, 2, \dots, \mathbb{N} = \mathbb{N}_+ \cup \{0\}$  be the sequence number of the occurrent event in the considered model. Denote by  $\mathbf{T} = (T_n)_{n \in \mathbb{N}}$  a sequence of independent time instants at which the IoT device detects the channel for packet transmission, where  $T_n$  is the time instant when the channel is detected for the  $n$ th time. Specifically, we define  $t < T_n \leq t + dt$ , where  $t$  is a discrete and integer time scale corresponding to the beginning of a time slot and  $dt$  is an infinitely short time interval. Denote by  $\mathbf{D} = \{0, 1\}$  a countable state space, where  $\mathbf{D} = 0$  represents the device detects an idle channel state, whereas  $\mathbf{D} = 1$  represents the device detects a busy one. Denote by  $\mathbf{o} = (o_n)_{n \in \mathbb{N}} = o(T_n)_{n \in \mathbb{N}}$  a sequence of conditionally independent channel detection results, where  $o_n$  is the  $n$ th detected channel state on the state space  $\mathbf{D}$  at time instant  $T_n$ . Due to the impact of noise and interference effects, there are underlying channel state hidden behind  $\mathbf{o}$ . Denote by  $\mathbf{H} = \{AF, FF, AB, FB\}$  the state space of the hidden channel state, where  $AF$  and  $FF$  represent the detection results are accurate and false, respectively, when the channel state is idle. In contrast, when the channel state is busy,  $AB$  and  $FB$  represent the detection results are accurate and false, respectively. Denote by  $\mathbf{C} = (C_n)_{n \in \mathbb{N}} = C(T_n)_{n \in \mathbb{N}}$  the successive hidden channel states at the time instant  $T_n$ , where  $C_n \in \mathbf{H}$ ,  $\mathbf{H} = (H_i)_{i \leq 4, i \in \mathbb{N}_+}$ . Denote by  $\tau = (\tau_n)_{n \in \mathbb{N}_+}$  a sequence of sojourn time in each hidden channel state, where  $\tau_n = T_n - T_{n-1}$ ,  $n \in \mathbb{N}_+$ . The basic structure of the proposed HSMM is illustrated in Fig. 2. The HSMM  $((\mathbf{C}, \mathbf{T}), \mathbf{o}) = ((C_n, T_n), o_n)_{n \in \mathbb{N}}$  is the extension of stochastic process  $(O_n)_{n \in \mathbb{N}}$  with the embedded hidden Markov chain  $(C_n, o_n)_{n \in \mathbb{N}}$  by allowing the underlying process to be a semi-Markov chain  $(C_n, T_n)_{n \in \mathbb{N}}$  with a sojourn time  $(\tau_n)_{n \in \mathbb{N}_+}$  for each state.

Denote by  $b(o_n) = P\{o_n | C_n = H_i\}$  the emission probability of  $o_n$  given the current hidden channel state  $H_i$  at  $T_n$ . Denote by  $a_{ij} = P\{C_n = H_i | C_{n-1} = H_j\}$  the transition probability of the embedded hidden Markov model from state  $H_j$  at  $T_{n-1}$  to state  $H_i$  at next time instant  $T_n$ , where  $i, j \leq 4, i, j \in \mathbb{N}_+$ . According to the IEEE 802.15.4 standard, the device waits for  $\tau_n$ , which follows uniform distribution, and then detects the channel state at  $T_n$ . Denote by  $f_{ij}(t)$

the probability density function (PDF) of the sojourn time  $\tau_n$  in a given state  $H_i$  conditioned on transferring from state  $H_j$ , where  $f_{ij}(\tau)d\tau = P\{\tau < T_n - T_{n-1} \leq \tau + d\tau | C_n = H_i, C_{n-1} = H_j\}$ . The probability that channel state  $C_{n-1}$  transits to state  $C_n$  at time  $T_n$  is  $P\{C_n = H_i, t < T_n \leq t + dt | C_{n-1} = H_j\}$ . Hence, denote by  $\alpha_i(t)dt$  the probability that the device predicts the hidden channel state  $H_i$  at the  $N$ th time instant  $T_N$  joint with all the historical detected channel states  $o_{\{0:N\}}$  from  $T_0$  to  $T_N$ , which is

$$\begin{aligned} \alpha_i(t)dt &= P\{C_N = H_i, t < T_N \leq t + \Delta t, O_{\{0:N\}}\} \\ &= \sum_{H_e \in \mathbf{H}} b(o_N) a_{ie} \int_0^t \alpha_e(t - \tau) f_{ie}(\tau) d\tau dt \quad (1) \end{aligned}$$

Suppose we have recorded all the detected channel states. We can calculate the maximum value of  $\alpha_i(T_N)dt$  at the time instant  $T_N$  under the condition of each state in  $\mathbf{H}$  with the historical states to find the most proper hidden channel state. The maximum probable hidden channel state is  $H_i = \operatorname{argmax}_{C_i \in \mathbf{H}, t \in \mathbf{T}} \alpha_i(t)$ , in which  $\alpha_i(T_N)dt$  refers to the probability of channel state  $C_N = H_i$  at time instant  $T_N$ . If the channel state is idle, we denote by  $\alpha_i(T_N)dt$  the corresponding channel access probability, otherwise we denote by  $1 - \alpha_i(T_N)dt$ . All the latent parameters,  $[\alpha_i, f_{ij}(t), b_i(o_n), a_{ij}]^T$ , can be iteratively learned by observations and acknowledgements based on the EM algorithm.

### C. Time-Sensitive Model

Consider the association mechanisms between the AP and devices while using the IEEE 802.15.4 carrier-sensing multiple access with collision avoidance (CSMA/CA) procedure. To control the packet BSD and prevent collisions with signals produced by other IoT devices, five coefficients are employed: the number of times that the device fails to access into the channel and starts a new back-off stage (NB<sub>-</sub>); the number of times the device detects the channel state (CW<sub>-</sub>); the back-off exponent (BE<sub>-</sub>), which initiates the timer of Backoff<sub>-</sub>; the waiting duration that the device has to wait before detecting the channel state (Backoff<sub>-</sub>); and the number of retransmission times (Retry<sub>1</sub>). The device counts down Backoff<sub>-</sub> to 0 from a number which is uniformly generated in the range  $[1, 2^{\text{BE}_-} - 1]$  and executes Clear Channel Assessment (CCA) procedure. The initial value of NB<sub>-</sub>, CW<sub>-</sub>, and BE<sub>-</sub> is set as 0, 2, and 3, respectively. The details of CSMA/CA procedure and parameter settings can be read from [17]. Suppose that all the devices are capable of detecting the channel state during CCA slots. After counting down the Backoff<sub>-</sub> which is initiated randomly according to the standard, the device will run the CCA procedure. The device has to perform twice CCA procedures before transmitting the packets. Both of the channel state detection results should be idle so that the device can enable the packet transmission. If either of the detection result is detected as busy, the device will increase BE<sub>-</sub>, initiate a random number between  $[1, 2^{(\text{BE}_-+1)} - 1]$  and start a new back-off stage. If the device fails to send the packet, it will reset NB<sub>-</sub> and BE<sub>-</sub> to 0 and 3 to begin a new back-off stage.

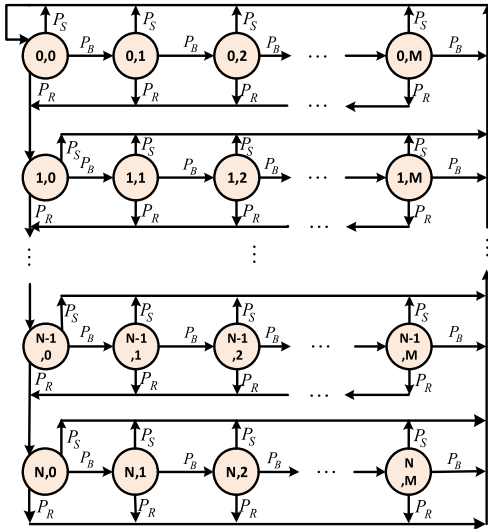


Fig. 3. Semi-Markov model with time-sensitive characteristics.

When building the model for the aforementioned CSMA/CA technique, time-sensitive variables such as packet back-off waiting process and the number of retransmissions should be considered. Assume that all devices are saturated. Denote by  $be(T_n)$  the stochastic process representing the number of  $BE_{-}$  for a given device. Denote by  $r(T_n)$  the stochastic process representing the number of  $Retry_{-}$  at  $T_n$ . Let  $\mathbf{E} = \{r(T_n) = i, be(T_n) = j\}$  be the state space of the bi-dimensional process, where  $0 \leq i \leq N$  and  $0 \leq j \leq M$ ,  $\{N | N \leq \max Retry_{-}\}$  is the maximum number of retransmission and  $\{M | M \leq \max BE_{-} - 3\}$  is the maximum number of back-off process. Note that the value of  $b(T_n)$  corresponds to  $BE_{-} - 3$  in the proposed model. Denote by  $\mathbf{X} = X(T_n)_{n \in \mathbb{N}} = (X_n)_{n \in \mathbb{N}}$  a sequence of random variable describing the state of the bi-dimensional process at time  $T_n$ . Let  $(\mathbf{X}, \mathbf{T}) = (X_n, T_n)_{n \in \mathbb{N}}$  be the semi-Markov chain with a sojourn time  $\{\tau_n | \tau_n = T_{n+1} - T_n, n \in \mathbb{N}\}$  for each state. Denote by  $\mathbf{S} = (S_{i,j})_{0 \leq i \leq N, 0 \leq j \leq M}$  the transition state of the semi-Markov model if the number of retransmission is  $i$  and the number of back-off exponent  $j$ , where  $(X_n, T_n)_{n \in \mathbb{N}} = (S_{i,j}, T_n)$ ,  $S_{i,j} = \{r(T_n) = i, b(T_n) = j\}$  and  $S_{i,j} \in \mathbf{E}$ . Fig. 3 shows the proposed semi-Markov model. In the proposed semi-Markov model, each state represents a back-off waiting process. After entering a state, the device remains in that state for a random time period determined by a uniform distribution with a pre-defined interval limit. In the semi-Markov model, if the device detects a busy channel state in either of the two channel assessments, it will not access the wireless channel. Instead, the device will transfer its back-off state to the next state to refresh the packet BSD with  $BE_{+} + 1$  but the  $Retry_{1-}$  will remain the same. Additionally, if the device successfully accesses the wireless channel but fails to send the packet, the device will proceed to the state with increased  $Retry_{1-}$  but the  $BE_{-}$  will be initialized as 3 corresponding to  $be(T_n) = 0$  in the semi-Markov model, and a new BSD for the packet will be generated. The device will return to state  $S_{0,0}$  in the semi-Markov model if it successfully accesses the wireless channel and sends the packet. Denote by

$\mu_1$  the probability of detecting a busy channel state at the first CCA. Denote by  $\mu_2$  the probability of detecting an idle one at the first CCA but a busy one at the second CCA. The  $\mu_1$  and  $\mu_2$  are

$$\mu_1 = a_i(T_N)$$

where  $TB = \operatorname{argmax}_{H_i \in \mathbf{H}} a_i(T_N)$  (2)

$$\mu_2 = a_k(T_{N+1})$$

where  $TB = \operatorname{argmax}_{H_k \in \mathbf{H}, C_i = TF} b(o(T_{n+1})) p_{ki} \int_0^t a_i f_{ki}(t - \tau) d\tau$  (3)

Following the semi-Markov model in Fig. 3, we denote by  $P_B$  the probability that the device detects a busy channel state and proceeds to the next back-off process. Let  $P_R$  be the probability that the device successfully accesses the channel but fails to transmit the packet. Denote by  $P_S$  the probability that the device successfully transmit the packet. All the proceeding transition probabilities in the semi-Markov model are

$$P_B = P(j, i | j, i - 1) = P(0, 0 | j, M)$$

$$= \mu_1 + (1 - \mu_1)\mu_2, 0 \leq i < M, 0 \leq j \leq N$$
 (4)

$$P_R = P(j, 0 | j - 1, i) = P(0, 0 | N, i)$$

$$= (1 - \mu_1)(1 - \mu_2)(1 - p), 0 \leq i \leq M, 0 \leq j < N$$
 (5)

$$P_S = P(0, 0 | j, i)$$

$$= (1 - \mu_1)(1 - \mu_2)p, 0 \leq i \leq M, 0 \leq j \leq N$$
 (6)

where  $p$  is the probability of the packet not acknowledged by an ACK message.

The packet BSD at a given state conditioned on the next transition state is derived from a uniform distribution determine by the back-off exponent  $BE_{-}$ . Let  $F_{S_{i_k}, S_{j_i}}(t)$  be the probability function of the sojourn time in a given state  $S_{j_i}$  with the next visiting state  $S_{i_k}$ , which is

$$F_{S_{i_k}, S_{j_i}}(t) = P\{T_{n+1} - T_n \leq t | X_{n+1} = S_{i_k}, X_n = S_{j_i}\}$$

$$= \begin{cases} 0, & t < 1 \\ \frac{t-1}{2^{BE_{-}+i-1}-1}, & 1 \leq t < 2^{BE_{-}+i-1} \\ 1, & t \geq 2^{BE_{-}+i-1} \end{cases}$$
 (7)

The PDF of  $F_{S_{i_k}, S_{j_i}}(t)$  can be given as:

- 1) If system transits into state  $S_{i_k}$  at time  $T_0$ , the PDF is
$$f_{S_{i_k}, 0}(t) dt = P\{t < T_0 < t + dt | X_0 = S_{i_k}\}$$
 (8)

- 2) If system transits into state  $S_{i_k}$  from state  $S_{j_i}$  at time  $T_n$ , the PDF is

$$f_{S_{i_k}, S_{j_i}}(t) dt = P\{t < T_n < t + dt | X_n = S_{i_k}, X_{n-1} = S_{j_i}\}$$
 (9)

Denote by  $\mathbf{q}$  the associate semi-Markov kernel.

$$\mathbf{q} = q_{S_{i_k}, S_{j_i}}(t)$$

$$= \lim_{dt \rightarrow 0} P\{X_n = S_{i_k}, t < T_n \leq t + dt | X_{n-1} = S_{j_i}\} / dt$$
 (10)

where  $S_{lk}, S_{ji} \in \mathbf{E}$  and  $t \geq 0$ . Then, the probability that the state  $S_{ji}$  transits to state  $S_{lk}$  during  $(t, t + dt)$  is  $q_{S_{lk}, S_{ji}} dt + o(dt)$ , where  $dt \rightarrow 0$  and  $o(dt)$  means the fact that probability to have the transition in the time  $dt$  is negligible with respect to  $q_{S_{lk}, S_{ji}} dt$ . Eq. 10 can be further extracted into the production between the state transition probability and the sojourn time PDF, which is

$$\begin{aligned} & q_{S_{lk}, S_{ji}} dt + o(dt) \\ &= P\{X_n = S_{lk}, t < T_n \leq t + dt | X_{n-1} = S_{ji}\} \\ &= P\{t < T_n \leq t + dt | X_n = S_{lk}, X_{n-1} = S_{ji}\} \\ &\quad \cdot P\{X_n = S_{lk} | X_{n-1} = S_{ji}\} \\ &= f_{S_{lk}, S_{ji}}(t) p_{S_{lk}, S_{ji}} dt + o(dt) \end{aligned} \quad (11)$$

where  $p_{S_{lk}, S_{ji}}$  is the transition probability from the state  $X_{n-1} = S_{ji}$  to state  $X_n = S_{lk}$ .

Let  $w_{S_{lk}, S_{ji}}(t) dt$  be the probability entering state  $S_{lk}$  during  $(t, t + dt)$  conditioned on transiting from state  $S_{ji}$ , where  $S_{ji}, S_{lk} \in \mathbf{E}$ , then (12), shown at the bottom of the next page. If  $X_0 = S_{ji}$ , then leaving state  $S_{ji}$  in interval  $(t, t + dt)$  is either:

- The system never leaves state  $S_{ji}$  before time  $t$  and emerges for the first time at  $(t, t + dt)$ , which is  $w_{S_{ji}, S_{ji}}(t) dt = f_{0, S_{ji}}(t) dt \delta_{S_{ji}, S_{lk}}$ .
- The system comes into state  $S_{lk}$  during  $(t, t + dt)$  conditioned on transiting from state  $S_{ef}$ , where the system stays for  $(t - \tau, t - \tau + dt)$  with the distribution as  $f_{S_{lk}, S_{ef}}(\tau) d\tau$ . Hence, by accumulating all medium transient states in this situation, we have  $\sum_{S_{ef} \in \mathbf{E}} p_{S_{lk}, S_{ef}} \int_0^t w_{S_{ef}, S_{ji}}(t - \tau) f_{S_{lk}, S_{ef}}(\tau) d\tau dt$ .

In short,  $w_{S_{lk}, S_{ji}}(t)$  can be summarized as:

$$\begin{aligned} w_{S_{lk}, S_{ji}}(t) dt &= f_{0, S_{ji}}(t) dt \delta_{S_{ji}, S_{lk}} \\ &\quad + \sum_{S_{ef} \in \mathbf{E}} p_{S_{lk}, S_{ef}} \int_0^t w_{S_{ef}, S_{ji}}(t - \tau) \\ &\quad \times f_{S_{lk}, S_{ef}}(\tau) d\tau dt \end{aligned} \quad (13)$$

The probability distributions of latency tail can be characterized by the maximum latency extreme values (EV) within a given time interval. The probability distribution of latency EV is related to its FPP. Suppose the relation between  $X_n$  and the corresponding  $\tau_n$  is  $\tau_n = T(X_n)$ , where  $\tau_n$  grows with the increase of  $X_n$  according to the backoff algorithm defined in IEEE standard 802.15.4. The EV probability is the probability that  $X_n \geq \xi$ , for a given  $\xi$ , such that  $\tau_n \geq T(\xi)$ . Thus, the maximum EV of the latency process  $T(X_n)$  is  $\mathcal{M}(t) = \max_{0 \leq n \leq N} (X_n)$ . The cumulative distribution function of EVs is  $F(\xi, t | X_0) = P\{\mathcal{M}(t) < \xi | X_0 = S_{ji}\}$ . Denote by  $\mathcal{T}(\xi) = \min_{\tau_n \neq 0} \{\tau_n | X_n = \xi\}$  the first passage time, which is the time required for transiting to state  $X_n = \xi$  for the first time. Since  $F(\xi, t | X_0)$  is the probability that  $X_n$  never crosses  $\xi$  during time  $0 \leq T(X_n) \leq t$ , it can be related to the first passage time, which is  $F(\xi, t | X_0) = P\{\mathcal{T}(\xi) > t | X_0 = S_{ji}\}$ . The relation between the probability distribution of the extreme latency tail and the first passage time can be expressed as  $P\{\mathcal{M}(t) < \xi | X_0 = S_{ji}\} = 1 - P\{\mathcal{T}(\xi) < t | X_0 = S_{ji}\}$ . Thus, if  $P\{\mathcal{T}(\xi) < t | X_0 = S_{ji}\}$  is minimized,  $P\{\mathcal{M}(t) <$

$\xi | X_0 = S_{ji}\}$  is maximized correspondingly. The probability density function of  $F(\xi, t | X_0)$  deduces that  $P\{\xi < \mathcal{M}(t) < \xi + d\xi | X_0 = S_{ji}\} = P\{t < \mathcal{T}(\xi) < t + dt | X_0 = S_{ji}\}$ . Denote by  $\mathfrak{T}_{S_{lk}, S_{ji}}(t)$  the average time required for the proposed semi-Markov process transitioning from the initial state  $S_{ji}$  to state  $S_{lk}$  for the first time, which corresponds to the FPT when the packet is successfully transmitted.

$$\begin{aligned} \mathcal{T}(\xi) &\Rightarrow \mathfrak{T}_{S_{lk}, S_{ji}}(t) \\ &= \inf\{u > 0 : X(t + u) = S_{lk} | X(t) = S_{ji}\} \quad \forall t \geq 0 \end{aligned} \quad (14)$$

Let  $g_{S_{lk}, S_{ji}}(t)$  be the PDF of  $\mathfrak{T}_{S_{lk}, S_{ji}}(t)$ , that is

$$\begin{aligned} g_{S_{lk}, S_{ji}}(t) dt &= P\{X(T_n) = S_{lk}, X(T_{i:i \in \{n-1, \dots, 1\}}) \neq S_{lk}, \\ &\quad \times t < T_n \leq t + dt | X(T_0) = S_{ji}\} \end{aligned} \quad (15)$$

which can be defined as the subtraction between two parts. The first part is the probability that after the  $n$ th time instant  $T_n$ , the system comes into state  $S_{lk}$  without any restriction, conditioned on the transition from state  $S_{ji}$ . The second part is the multiplication between the probability that after the  $m$ th time instant  $T_m$ , the system first comes to state  $S_{lk}$  conditioned on transiting from state  $S_{ji}$ , and the probability that the system comes to state  $S_{lk}$  without any restriction conditioned on transiting from state  $S_{lk}$ . Thus, we have  $g_{S_{lk}, S_{ji}}(t) dt$  in Eq. 16, shown at the bottom of the next page. The probability that the system first comes to state  $S_{lk}$  conditioned on transiting from state  $S_{ji}$  after the  $m$ th time instant  $T_m$  can be defined as  $w_{S_{lk}, S_{lk}}(\tau)$  which equals to  $P\{X_n = S_{lk}, \tau < T_n - T_m < \tau + d\tau | X_m = S_{lk}\}$ . Hence, based on Eq. 16, FPP can be expressed as:

$$\begin{aligned} g_{S_{lk}, S_{ji}}(t) &= w_{S_{lk}, S_{ji}}(t) - \sum_{\substack{m=1 \\ X_m=S_{lk}}}^{n-1} \int_0^t w_{S_{lk}, S_{lk}}(\tau) \\ &\quad \cdot g_{S_{lk}, S_{ji}}(t - \tau) d\tau \end{aligned} \quad (17)$$

Fig. 4 shows a case study of the simulation results of the FPP to successfully send the packet conditioned on initiating from each state in the proposed semi-Markov model. The FPP is the maximum probability of a packet being successfully transmitted in a given backoff sojourn duration. We evaluate the FPP within  $dt$  based on the PDF of FPT. We set the maximum limitation of `maxBE_` to 3 and `maxRetry_` to 3, respectively. Fig. 4 shows that the packet can always wait for a proper BSD (x-coordinate of each subfigure) thereby achieve the maximum value of FPP. For example, the subfigure in the top row and first column shows that, if the device initiates from the state  $S_{00}$ , the device can successfully transmit the packet with the maximum probability after waiting for a proper BSD (20ms). In addition, as shown in Fig. 4, if the device detects a busy channel, the proper packet BSD for the maximum FPP increases with the growth in `BE_`. Moreover, retransmission has modest impact on the packet BSD corresponding to the maximum FPP. Also note that, when the device continues to detect a busy channel, the maximum FPP to successfully transmit the packet decreases gradually.

#### IV. PROBLEM FORMULATION

As shown in Fig. 4, the proper decision on the packet BSD,  $t$ , can be obtained by maximizing the FPP in Eq. 17. In this section, we first investigate the concavity property of Eq. 17. Then, we formulate the problem of minimizing the average packet sojourn time based on the accumulation of all the determined BSD corresponding to the maximum FPP in each transmission cycle.

*Lemma 1: Function  $g_{S_{lk}, S_{ji}}(t)$  is concave if time  $t$  is in a convex set.*

*Proof:* Refer to Appendix A.  $\square$

We can conclude that there is always a  $t^*$  satisfying  $t^* \in \operatorname{argmax}_t g_{S_{lk}, S_{ji}}(t)$ . Refer to  $g_{S_{lk}, S_{ji}}(t)$  as  $g_n(t)$  the FPP at time instant  $T_n$ . Denote by  $\hat{g}_n(t)$  the probability that at transmission cycle  $n$ , the device detects an idle channel state, generates the packet BSD corresponding to the maximum FPP, and then sends the packet until the BSD is counted down to zero, but unsuccessfully transmits the packets. Thus,  $\hat{g}_n(t)$  can be expressed as

The average packet BSD at the  $n$ th transmission cycle is

$$\begin{aligned} n = 1, \quad D_1 &= t_1 g_1(t) \\ t_1 &\in \operatorname{argmax}_t g_1(t), \quad t_1 < T \\ n > 1, \quad D_n &= t_1 \hat{g}_1(t_1) + t_2 \hat{g}_1(t_1) \hat{g}_2(t_2) + \dots \\ &\quad + t_n \prod_{i=1}^{n-1} \hat{g}_i(t_i) g_n(t) \\ t_{n \in \{1, \dots, n\}} &\in \operatorname{argmax}_t g_{n \in \{1, \dots, n\}}(t), \quad \sum_n t_n < T \end{aligned} \quad (19)$$

where we define that the accumulative summation of all the historical packet BSD should be smaller than a pre-determined time limitation  $T$ . Based on Eq. 19, our objective is to minimize the average packet sojourn time, which can be expressed as  $\operatorname{argmin}_t \sum_n D_n$ . We provide quadratic penalty function as the augment element to constrain the sum of all

the BSD. Please refer to Appendix B for more details. Then, the objective function is

$$\begin{aligned} \operatorname{argmin}_t \quad & \sum_{i=1}^n (1 - g_i(t) + B_i t_i g_i(t_i) + (n - i) A_i) \\ & + \frac{\varepsilon}{2} \left\| \sum_{i=1}^n t_i - T \right\|^2 \\ \text{s.t.} \quad & B_i = \prod_{j=1}^{i-1} \hat{g}_j(t_j), \quad A_i = \prod_{j=1}^i \hat{g}_j(t_j) \\ & t_{i \in \{1, \dots, n\}} \in \operatorname{argmax}_t g_{i \in \{1, \dots, n\}}(t), \quad \sum_{i=1}^n t_i < T \end{aligned} \quad (20)$$

*Lemma 2: Each BSD iteration are forced to keep away from the proposed latency boundary if the positive penalty coefficient  $\varepsilon$  is less than  $(1 - B_i t_i) \nabla_{t_i}^2 g_i(t_i) - 2B_i \nabla_{t_i} g_i(t_i)$ .*

*Proof:* Refer to Appendix B.  $\square$

Our objective is to find the optimal packet BSD for the packet corresponding to the maximum FPP to successfully transmit the packet in the current transmission cycle. In a nutshell, first we determine the hidden channel state based on the state with the maximum probability which is calculated from the proposed channel detection method, and further use the corresponding channel access probability as the state transition probability in the proposed TSM. Then, considering the FPP conditioned on beginning from the  $n$ -th transmission cycle, we investigate the optimum packet BSD corresponding to the maximum FPP. We assume that the packet sojourn time should not exceed the delay restriction of the time-sensitive industrial applications. We design a constrained objective function based on the penalty method by taking the mean of the packet sojourn time. Specifically, the proposed function is composed of the original objective function plus one additional barrier for the constraint, which is positive when the current produced BSD make the overall packet sojourn time violate

$$\begin{aligned} & w_{S_{lk}, S_{ji}}(t) dt \\ &= P\{X_n = S_{lk}, t < T_n \leq t + dt | X_0 = S_{ji}\} \\ &= P\{X_n = S_{lk}, X_{\{n-1, \dots, 1\}} = S_{ji}, t < T_n \leq t + dt | X_0 = S_{ji}\} \\ &\quad + \underbrace{\sum_{S_{ef} \in \mathbf{E}} P\{X_n = S_{lk}, \tau < T_n - T_{n-1} \leq \tau + d\tau | X_{n-1} = S_{ef}\}}_{f_{S_{ef}, S_{lk}}(\tau) d\tau p_{S_{ef}, S_{lk}}} \\ &\quad \cdot P\{X_{n-1}, t - \tau < T_{n-1} \leq t - \tau + d\tau | X_0 = S_{ji}\} \end{aligned} \quad (12)$$

$$\begin{aligned} g_{S_{lk}, S_{ji}}(t) dt &= P\{X_n = S_{lk}, t < T_n < t + dt | X_0 = S_{ji}\} \\ &\quad - \sum_{m=1}^{n-1} P\{X_n = S_{lk}, t - \tau < T_n - T_m < t - \tau + dt | X_m = S_{lk}\} \\ &\quad \cdot \underbrace{P\{X_m = S_{lk}, X_{n-1} \neq S_{lk}, \dots, X_1 \neq S_{lk}, \tau < T_m \leq \tau + d\tau | X_0 = S_{ji}\}}_{g_{S_{lk}, S_{ji}}(t - \tau) d\tau} \end{aligned} \quad (16)$$

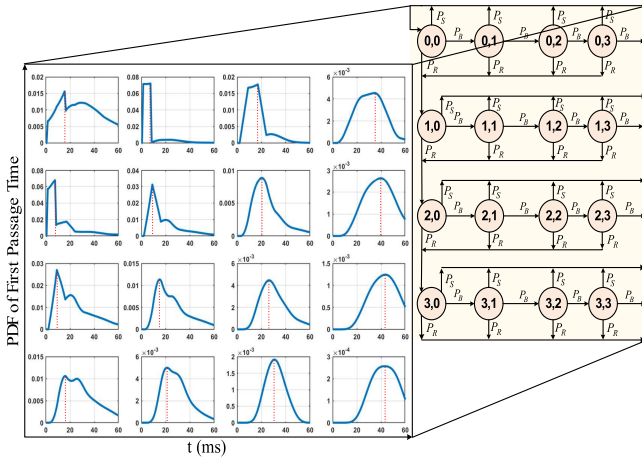


Fig. 4. The FPP of a 4x4 TSM.

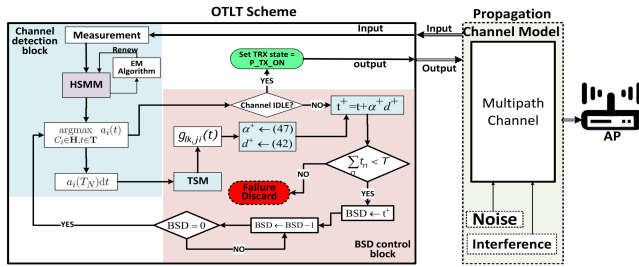


Fig. 5. Overview of the OTLT Scheme.

the delay constraint and zero otherwise. By multiplying a positive coefficient to the penalty terms, we penalize constraint violations more severely with a larger coefficient, thereby force the minimizer of the penalty function to get closer to the feasible region of the packet sojourn time.

## V. OPTIMAL TRANSMISSION LATENCY TAMING SCHEME

As depicted in Fig. 5, the OTLT scheme consists of a channel detection module and a packet BSD control module. In the channel detection module, we investigate all of the unknown parameters in the proposed HSMM using the EM algorithm in Alg. 1, where the observations utilized to correct these unknown parameters are collected from real-life detection measurements in an industrial environment. Based on the derived HSMM, we utilize Alg. 2 to estimate the hidden channel state with the current detected observations and compute the corresponding channel access probability  $a_i(T_N)dt$ . In the packet BSD control module, considering the collision avoidance procedure, the obtained channel access probability is then utilized to build the TSM. The maximum FPP shown in Eq. 17 is investigated in accordance with the proposed

### Algorithm 1 Expectation Maximum Parameter Estimation

**Require:** Observation set  $\mathbf{o} = o_{n=1:N}$ ;  
Hidden Channel States  $\mathbf{C} = C_{n=1:N}$ ;  
Time instants  $\mathbf{T} = T_{n=1:N}$ ; Sojourn time  
 $\tau = \tau_{n=1:N-1} = \{T_2 - T_1, \dots, T_N - T_{N-1}\}$   
**Ensure:**  $\pi_i; i \in \mathbb{E}$ ,  $f_{i,i} \in \mathbb{E}(t)$ ,  $a_{j,i}; j, i \in \mathbb{E}$ ,  $f_{j,i}; j, i \in \mathbb{E}(t)$ ,  
 $b_{j,j} \in \mathbb{E}(O_{n;n=1:N})$ .  
1: **initiate:**  $\eta = 0$   
2: **for each**  $i \in \mathbb{E}$  **do**  
3:  $\pi_i \leftarrow \frac{1}{\text{Size of } \mathbb{E}}$ ,  $f_{i,i} \in \mathbb{E}(t) \leftarrow \sum_{n=1}^N \frac{\{\tau_n: C_n=i\}}{T_N}$ ,  
 $b_j(o_n) \leftarrow \frac{\#\{o_n: C_n=j\}}{N}$   
4: **for each**  $j \in \mathbb{E}$  **do**  
5:  $p_{ji} \leftarrow \frac{\#\{n: C_{n+1}=j | C_n=i\}}{N}$ ,  
 $f_{ji}(t) \leftarrow \sum_{n=1}^N \frac{\{\tau_n: C_{n+1}=j | C_n=i\}}{T_N}$ ,  
6: **end for**  
7: **end for**  
8:  $\eta \leftarrow \eta + 1$   
9: **repeat**  
10:  $[\pi_i, f_{i,i}(d_i), a_{j,i}, f_{j,i}(t), b_i(o_t = j)] \leftarrow \text{Eq. 23-Eq. 27}$ ,  
11: **until**  $Q(\boldsymbol{\theta}, \boldsymbol{\theta}^{(\eta+1)}) - Q(\boldsymbol{\theta}, \boldsymbol{\theta}^{(\eta)}) < \epsilon$   
12: **return**  $\pi_i; i \in \mathbb{E}$ ,  $f_{i,i} \in \mathbb{E}(t)$ ,  $a_{j,i}; j, i \in \mathbb{E}$ ,  $f_{j,i}; j, i \in \mathbb{E}(t)$ ,  
 $b_{j,j} \in \mathbb{E}(O_{n;n=1:N})$ .

TSM. A cumulative summation of each BSD in consideration of the quadratic penalty latency constraints is formulated to calculate the gradient of the BSD control function  $d_n$  and the corresponding control scale  $\alpha_n$ . The BSD for the next transmission cycle is renewed by  $t_i^{n+1} = t_i^n + \alpha_i^{n+1} d_i^{n+1}$ . The OTLT scheme counts down BSD to 0 and then returns to the channel detection module re-estimate the hidden channel state using Alg. 2. Alg. 3 explains the OTLT scheme in more detail.

### A. Parameter Estimation in HSMM

The EM algorithm is a broadly applicable approach to the iterative computation of maximum likelihood (ML) estimation, useful in variety of incomplete data problems [27]. We introduce a complete data set  $\{\mathbf{o}, \mathbf{C}, \mathbf{T}\}$  with  $\mathbf{o} = [o_1, \dots, o_N]^T$ ,  $\mathbf{C} = [C_1, \dots, C_N]^T$ ,  $\mathbf{T} = [T_1, \dots, T_N]^T$ ,  $\boldsymbol{\tau} = [\tau_1, \dots, \tau_{N-1}]^T = [T_2 - T_1, \dots, T_N - T_{N-1}]$ . The complete data log-likelihood function can be easily expressed as  $\ln(Q(\boldsymbol{\theta}, \boldsymbol{\theta}')) = \ln(\prod_{\mathbf{C}} \prod_{\boldsymbol{\tau}} P(\mathbf{o}, \mathbf{X} | \boldsymbol{\theta}) P(o_{1:N}, C_{1:N} | \boldsymbol{\theta}^{(\eta)}))$ , where  $\boldsymbol{\theta}$  is the estimation parameter set of  $[\pi_{C_0}, f_{C_0}(t), a_{C_{n+1}, C_n}, f_{C_{n+1}, C_n}(t), b_{C_n}(o_n)]^T$ ,  $\boldsymbol{\theta}^{(\eta)}$  is the parameter set obtained from the  $\eta$ th iteration. In  $\boldsymbol{\theta}$ ,  $\pi_{C_0}$  is the stationary probability at time instant  $T_0$  under the state  $C_0$ ;  $f_{C_0}(t)$  is the PDF of sojourn time at the state  $C_0$ ;

$$\begin{aligned} \hat{g}_n(t) &= P\{X(T_n) = S_{lk}, X(T_{n-1}) \neq S_{lk}, \dots, X(T_1) \neq S_{lk}, t < T_n \leq t + dt | X(T_0) = S_{ji}\} \\ &= \sum_{\substack{X(T_n) \neq S_{lk} \\ X(T_n) \in \mathbb{E}}} \left[ w_{S_{lk}, S_{ji}}(t) - \sum_{\substack{m=1 \\ X(T_m) = S_{lk}}}^{n-1} \int_0^t w_{S_{lk}, S_{lk}}(\tau) \cdot g_{S_{lk}, S_{ji}}(t - \tau) d\tau \right] \end{aligned} \quad (18)$$

$a_{C_{n+1}, C_n}$  is the transition probability from state  $C_n$  to state  $C_{n+1}$  during time duration  $T_{n+1} - T_n$ ;  $f_{C_{n+1}, C_n}(t)$  is the PDF of sojourn time when transiting from state  $C_n$  to state  $C_{n+1}$ ;  $b_{C_n}(o_n)$  is the emission probability from the hidden state  $C_n$  to the observation  $o_n$  at time instant  $T_n$ . The idea behind the EM criterion is to estimate  $\theta$  iteratively in two steps: an expectation (E)-step and a maximization (M)-step. In the first step,  $\ln(Q(\theta, \theta^{(\eta)}))$  is taken with respect to the conditional probability of the latent variables. In the second step, the conditioned expectation is decomposed and maximized with respect to the parameters of interest. The two steps iterate until a predetermined convergence condition is met. In the following, we explain the calculation flow and present the EM algorithm in Alg. 1.

**E-step:** Considering the preceding expression (1), we have the objective function as

$$\ln Q(\theta, \theta^{(\eta)}) = \sum_{\mathbf{C} \in \mathbb{E}} \sum_{\tau \in \mathcal{T}} \log \left( \pi_{C_0} f_{C_0} \prod_{n=1}^{N-1} a_{C_n C_{n+1}} \cdot f_{C_n C_{n+1}}(t - \tau_n) b_{C_n}(o_n) \right) P(\mathbf{o}, \mathbf{C} | \theta^{(\eta)}) \quad (21)$$

**M-step:** Derived from Eq. 21, we estimate the hidden parameters by exploring the maximum problem on the  $(\eta)$ th iteration:

$$\begin{aligned} & \underset{\theta}{\operatorname{argmax}} \ln Q(\theta, \theta^{(\eta)}) \\ & \text{s.t. } \sum_i \pi_i = 1, \sum_t f_{ji}(t) = 1, \\ & \quad \times \sum_i a_{ji} = 1, \sum_j b_i(j) = 1 \end{aligned} \quad (22)$$

Solving Eq. 22, the stationary probability  $\pi_{C_0}$ , the PDF of sojourn time  $f_{C_0}(t)$ , the transition probability  $a_{C_{n+1}, C_n}$  of the proposed HSMM, the PDF of sojourn time  $f_{C_{n+1}, C_n}(t)$ , and the emission probability  $b_{X_n}(o_n)$  can be calculated as

Considering Eq. 23 – Eq. 27, shown at the bottom of the next page, the proposed EM parameter estimation algorithm is summarized in Alg. 1. Alg. 2 shows the pseudocode of the proposed forward algorithm method for hidden channel state detection. Given the observation sequence, the embedded Markov transition matrix, the sojourn time distribution of each state and the emission transition probability of the observation, when the packet BSD count down to zero, Alg. 2 outputs the forward probability  $\alpha_{C_N}(T_N)$  and also the most likely hidden channel state  $C_N$  by calculating the maximum likelihood of all the hidden states over the historical detection results. In this way, by tracking the hidden state with the highest likelihood in each step, the hidden channel state at time instant  $T_N$  can be discovered.

### B. Packet BSD Control Gradient

Denote by  $d_i$  the control gradient and further suppose  $z_i - t_i = d_i$ . We define a quadratic function of  $z_i - t_i$  with

---

### Algorithm 2 Forward Algorithm-Based Hidden Channel Detection

---

**Require:** Observation set,  $\mathbf{o}$ ; Steady state probability,  $\pi$ ; Sojourn time distribution,  $\mathbf{f}(t)$ ; Steady state Sojourn time distribution,  $\mathbf{f}_\pi(t)$ ; Transition matrix,  $\mathbf{p}$ ; Emission transition probability,  $\mathbf{b}(\mathbf{o})$

**Ensure:** Hidden channel state  $C_N$ . Related probability  $\alpha_{C_N}(T_N)$

- 1: **for** each state  $i \in \mathbf{H}$  **do**
- 2:    $\alpha_i(T_0) \leftarrow b_i(o(T_0)) \pi_i f_{\pi_i}(t)$ ;
- 3:    $C_i \leftarrow 0$ ;
- 4: **end for**
- 5: **for** each time step  $n \in \{1, \dots, N\}$  **do**
- 6:   **for** each state  $C_n \in \mathbf{H}$  **do**
- 7:      $\alpha_{C_n}(T_n) \leftarrow \max_{s \in \mathbf{H}} b_{C_n}(o_n) p_{s, C_{n-1}} \int_0^{T_n - T_{n-1}} \alpha_{C_{n-1}}(T_{m-1} + \tau) f_{s, C_{n-1}}(\tau) d\tau$ ;
- 8:      $C_n \leftarrow \operatorname{argmax}_{C_n \in \mathbf{H}} b_{C_n}(o_n) p_{s, C_{n-1}} \int_0^{T_n - T_{n-1}} \alpha_{C_{n-1}}(T_{n-1} + \tau) f_{s, C_{n-1}}(\tau) d\tau$ ;
- 9:   **end for**
- 10: **end for**
- 11: **return**  $[C_N, \alpha_{C_N}(T_N)]$

---

the constrained of  $\bar{\mathcal{J}}(t_i, \mu)$ , which is defined in Eq. 44, as

$$\begin{aligned} & \min_{z_i} \frac{1}{2} (z_i - t_i)' \mathcal{H} (z_i - t_i) + (z_i - t_i) \nabla_{t_i} \bar{\mathcal{J}}(t_i, \mu) + \bar{\mathcal{J}}(t_i, \mu) \\ & \text{s.t. } (z_i - t_i) \nabla_{t_i} \bar{\mathcal{J}}(t_i, \mu) \leq 0 \\ & \Rightarrow \min_{z_i} \frac{1}{2} (z_i - t_i)' \mathcal{H} (z_i - t_i) + (z_i - t_i) \left( \nabla_{t_i} g_i(t_i) (B_i t_i - 1) \right. \\ & \quad \left. + B_i g_i(t_i) + \max [\varepsilon (\sum_{i=1}^n t_i - T) + \mu, 0] \varepsilon d_i \right) \\ & \text{s.t. } (z_i - t_i) \nabla \bar{\mathcal{J}}(t_i, \mu) \leq 0 \end{aligned} \quad (28)$$

where  $\mathcal{H}$  is a positive definite symmetric matrix, which can be given as  $(0, 1)$ -matrices to simplify the calculation complexity. Substituting Eq. 44 in Appendix B into Eq. 28 and taking integrative with respect to  $z$ , we can obtain the BSD control gradient as

$$0 = (z_i - t_i) \mathcal{H} + \left( \nabla_{t_i} g_i(t_i) (B_i t_i - 1) + B_i g_i(t_i) + \max [\varepsilon (\sum_{i=1}^n t_i - T) + \mu, 0] c d_i^n \right) \quad (29)$$

$$d_i^{n+1} = z_i - t_i \quad (30)$$

$$\begin{aligned} & = - \frac{\left( \nabla_{t_i} g_i(t_i) (B_i t_i - 1) + B_i g_i(t_i) \right) \mathcal{H}^T}{\mathcal{H} \mathcal{H}^T} \\ & \quad - \frac{\max [\varepsilon (\sum_{i=1}^n t_i - T) + \mu, 0] c d_i^n \mathcal{H}^T}{\mathcal{H} \mathcal{H}^T} \end{aligned} \quad (31)$$

### C. Packet BSD Control Scale

Considering descent lemma, the difference between  $\bar{\mathcal{J}}(t_i^n + \alpha_i^n d_i^{n+1}, \mu)$  and  $\bar{\mathcal{J}}(t_i^n, \mu)$  is

$$\begin{aligned} & \bar{\mathcal{J}}(t_i^n + \alpha_i^n d_i^{n+1}, \mu) - \bar{\mathcal{J}}(t_i^n, \mu) \\ & \leq \int_0^{\alpha_i^n} d_i^{n+1} \nabla_{t_i} \bar{\mathcal{J}}(t_i^n + \alpha_i^n d_i^{n+1}, \mu) d\alpha_i^n \\ & \quad + \left| \int_0^{\alpha_i^n} d_i^{n+1} (\nabla_{t_i} \bar{\mathcal{J}}(t_i^n + \alpha_i^n d_i^{n+1}, \mu) \right. \\ & \quad \left. - \nabla_{t_i} \bar{\mathcal{J}}(t_i^n, \mu) d\alpha_i^n \right| \\ & \leq \alpha_i^n \nabla_{t_i} \bar{\mathcal{J}}(t_i^n, \mu) d_i^{n+1} + \|d_i^{n+1}\| \int_0^{\alpha_i^n} L_i^n \alpha_i^n \|d_i^{n+1}\| d\alpha_i^n \\ & = \alpha_i^n \nabla_{t_i} \bar{\mathcal{J}}(t_i^n, \mu) d_i^{n+1} + \frac{1}{2} \alpha_i^n L_i^n \|d_i^{n+1}\|^2 \end{aligned} \quad (32)$$

where  $d_n$  is the changing direction of the packet BSD at the  $n$ th transmission cycle,  $L_n$  is some scalar which satisfies

$$L_i^n \geq \frac{\bar{\mathcal{J}}(t_i^n + \alpha_i^n d_i^{n+1}, \mu) - \bar{\mathcal{J}}(t_i^n, \mu)}{\alpha_i^n \|d_i^{n+1}\|} \quad (33)$$

Taking derivative of Eq. 32 with respect to  $\alpha_n$ , we have the optimal step size,  $\bar{\alpha}$ , based on descent direction  $d_n$ , that is

$$\begin{aligned} & \min_{\alpha_i^n} \alpha_i^n \nabla_{t_i} \bar{\mathcal{J}}(t_i^n, \mu) d_i^{n+1} + \frac{1}{2} \alpha_i^n L_i^n \|d_i^{n+1}\|^2 \\ & \text{s.t. } \alpha_i^n \geq 0 \end{aligned} \quad (34)$$

Solving Eq. 34, we obtain

$$\begin{aligned} & \alpha_i^{n+1} \\ & = \frac{(\mathcal{V} + \max[\varepsilon(\sum_{i=1}^n t_i - T) + \mu, 0]) d_i^{n+1}}{L_i^n \|d_i^{n+1}\|^2} \end{aligned} \quad (35)$$

where  $\mathcal{V} = \nabla_{t_i} g_i(t_i)(B_i t_i - 1) + B_i g_i(t_i)$ . Combining Eq. 31 and Eq. 35, we have

$$t_i^{n+1} = t_i^n + \alpha_i^{n+1} d_i^{n+1} \quad (36)$$

Alg. 3 shows the overall scheme to obtain the optimal back-off time for the next transmission cycle. Given the distribution of the FPT,  $g_i(t)$ , its inverse,  $\hat{g}_i(t)$ , and a positive definite symmetric matrix, the algorithm outputs the best packet BSD,  $t_i^{n+1}$ . Step 12 in Alg. 3 wraps up the objective

### Algorithm 3 Optimal Transmission Latency Taming

**Require:** Positive Definite Symmetric Matrix  $\triangleq H$ ;  
First Passage Time Distribution  $\triangleq g_i(t)$ ;

**Ensure:** The Optimal Packet BSD  $t_i^{n+1}$

- 1:  $n \leftarrow 0$ ,  $\alpha^n \leftarrow \mathbf{vec}[0]_{1:n}$ ,  $d^n \leftarrow \mathbf{vec}[0]_{1:n}$ ,  
 $\mu^n \leftarrow \mathbf{vec}[1]_{1:n}$ ,  $\varepsilon \leftarrow 100$ ,
- 2: Randomly Initial  $t_i^0 \leftarrow \text{rnd}[1, 2^{\text{BE}} - 1]$
- 3: Initial CSMA/CA
- 4: [Channel, Transition\_Probability]  $\leftarrow$  Alg. 2
- 5: **if** Channel == **Idle** **then**
- 6: TX == ON
- 7: **else**
- 8: **repeat**
- 9:  $\mathcal{J}(t, z, \mu) \leftarrow$  Eq. 44
- 10:  $d_i^{n+1} \leftarrow$  Eq. 31,  $\alpha_i^{n+1} \leftarrow$  Eq. 35
- 11:  $t_i^{n+1} \leftarrow$  Eq. 36,  $\mu^{k+1} \leftarrow$  Eq. 45
- 12: Initial CSMA/CA
- 13: **if** Channel == **Idle** **then**
- 14: TX == ON
- 15: **else**
- 16: CONTINUE
- 17: **end if**
- 18: **until**  $n > \text{maxMacCSMABack-off}$
- 19: **end if**
- 20: **return**  $t_i^{n+1}$

function with the average packet sojourn time in Eq. 40 and the quadratic delay barrier in Eq. 46 which is used to limit the transmission delay. Then, the optimal control gradient in the current transmission cycle is calculated based on the objective function. The optimal control scale is obtained in Step 14, which can yield a delay reduction along the control gradient. Note that the average packet sojourn time is renewed in each transmission cycle. To tame the distribution tail of the packet sojourn time, the proposed OTLT scheme investigates the best BSD control gradient and the corresponding scale on the current channel access probability and the FPP distribution of packet BSD. Therefore, the packet sojourn time can be limited within a determined delay bound.

$$\pi_i = \frac{P(\mathbf{o}, C_0 = i | \boldsymbol{\theta}^{(n)})}{P(\mathbf{o} | \boldsymbol{\theta}^{(n)})} \quad (23)$$

$$f_{C_0}(d_e) = \frac{P(\mathbf{o}, C_0 = e, \tau_0 = d_e | \boldsymbol{\theta}^{(n)})}{P(\mathbf{o}, C_0 = i | \boldsymbol{\theta}^{(n)})}, \quad (24)$$

$$a_{ji} = \frac{\sum_{n=1}^{N-1} P(\mathbf{o}, C_{n+1} = i, C_n = j | \boldsymbol{\theta}^{(n)})}{\sum_{n=1}^{N-1} P(\mathbf{o}, C_n = i | \boldsymbol{\theta}^{(n)})} \quad (25)$$

$$f_{ji}(t) = \frac{\sum_{n=1}^N P(\mathbf{o}, C_{n+1} = j, C_n = i, \tau < T_{n+1} - T_n < \tau + d\tau | \boldsymbol{\theta}^{(n)})}{\sum_{n=1}^N \sum_{\tau \in \mathcal{T}} P(\mathbf{o}, C_{n+1} = j, C_n = i, \tau < T_{n+1} - T_n < \tau + d\tau | \boldsymbol{\theta}^{(n)})} \quad (26)$$

$$b_i(o_t = j) = \frac{\sum_{n=1}^N \left( \sum_{\tau \in \mathcal{T}} P(o, C_n = i, \tau < T_{n+1} - T_n < \tau + d\tau | \boldsymbol{\theta}^{(n)}) \delta_{o_i j} \right)}{\sum_{n=1}^N \sum_{\tau \in \mathcal{T}} P(o, C_n = i, \tau < T_{n+1} - T_n < \tau + d\tau | \boldsymbol{\theta}^{(n)})} \quad (27)$$

#### D. Discussion

The produced tail taming problem is solved by introducing the multiplier method, where the quadratic penalty term is added to the Lagrangian function of the objective function. We show that when the penalty function is of quadratic, the sequence of objective function outcomes generated by the multiplier method converges to the finest quality point at a linear rate proportional to the number of iterations as the number of iterations increases. It implies that the multiplier method can significantly reduce the computation time. The proving steps are as follows.

We simplify Eq. 40 and Eq. 45, which results in  $t^{k+1} = \operatorname{argmin}_t \{g(t^k) - (\mu^k)^T(Qt^k - p) + \frac{\varepsilon^k}{2}\|Qt^k - p\|^2\}$  and  $\mu^{k+1} = \mu^k - \varepsilon^k(Qt^{k+1} - p)$ , where  $Q$  and  $p$  are matrix penalty parameter of the proposed penalty function,  $k$  is the  $k$ -th iteration of the proposed penalty method. Note that the Lagrange function of the problem is  $\mathcal{G}(t, \mu) = g(t) - \mu^T(Qt - p)$ . A pair  $(t, \mu) \in \mathcal{T} \times \mathbb{R}^m$  is dual feasible if and only if  $(t' - t)^T(\nabla g(t) - Q^T\mu + Q^T\varepsilon(Qt - p)) \geq 0, \forall t' \in \mathcal{T}$ . Set  $t = t^{k+1}$  and substitute  $\mu^{k+1} = \mu^k - \varepsilon^k(Qt^{k+1} - p)$  into the above variational inequality, we have  $(t' - t)^T(\nabla g(t) - Q^T\mu + Q^T\varepsilon(Qt - p)) = (t' - t^{k+1})^T(\nabla g(t^{k+1}) - Q^T\mu^{k+1}) \geq 0$ , where  $\forall t \in \mathcal{T}$ . Using the convexity of function  $g(t)$  we obtain

$$\begin{aligned} & \mathcal{G}(t^{k+1}, \mu^{k+1}) - \mathcal{G}(t, \mu) \\ & \geq \mu^T Q(t^{k+1} - t) + \mu^T(Qt - p) - (\mu^{k+1})^T(t^{k+1} - t) \\ & = \|\mu^k - \mu^{k+1}\|^2(\varepsilon^k)^{-1} + (\mu - \mu^k)^T(\varepsilon^k)^{-1}(\mu^k - \mu^{k+1}) \end{aligned} \quad (37)$$

By setting  $(t, \mu) = (t^*, \mu^*)$ , in which  $(t^*, \mu^*)$  is dual feasible solutions, Eq. 37 can be turned into  $(\mu^k - \mu^*)^T(\varepsilon^k)^{-1}(\mu^k - \mu^{k+1}) \geq \|\mu^k - \mu^{k+1}\|^2(\varepsilon^k)^{-1} + (\mathcal{G}(t^*, \mu^*) - \mathcal{G}(t^{k+1}, \mu^{k+1}))$ . Using the above inequality, the sequence  $\{\mathcal{G}(t^*, \mu^*) - \mathcal{G}(t^{k+1}, \mu^{k+1})\}$ , which can be used to explain the rationale of estimating the convergence rate of the proposed quadratic penalty function method, has the features like  $\|\mu^{k+1} - \mu^*\|^2(\varepsilon^k)^{-1} \leq \|(\mu^k - \mu^*)\|^2(\varepsilon^k)^{-1} - \|(\mu^k - \mu^{k+1})\|^2(\varepsilon^k)^{-1} - 2(\mathcal{G}(t^*, \mu^*) - \mathcal{G}(t^{k+1}, \mu^{k+1}))$ . Using the fact  $\mathcal{G}(t^*, \mu^*) - \mathcal{G}(t^{k+1}, \mu^{k+1}) \geq 0$  and summing this relation over  $j = 0, \dots, k-1$ , we can have

$$\begin{aligned} & 2 \left( \sum_{j=0}^{k-1} \mathcal{G}(t^{j+1}, \mu^{j+1}) - k\mathcal{G}(t^*, \mu^*) \right) \\ & \geq \|(\mu^k - \mu^*)\|^2(\varepsilon^k)^{-1} - \|(\mu^0 - \mu^*)\|^2(\varepsilon^0)^{-1} \\ & \quad + \sum_{j=1}^{k-1} \|(\mu^j - \mu^{j+1})\|^2(\varepsilon^j)^{-1} \end{aligned} \quad (38)$$

Considering Eq. 42, let  $k = j$ ,  $(t, \mu) = (t^j, \mu^j)$ , we have  $2j\mathcal{G}(t^{j+1}, \mu^{j+1}) - \mathcal{G}(t^j, \mu^j) \geq 2j\|(\mu^j - \mu^{j+1})\|^2(\varepsilon^j)^{-1}$ . Summing Eq. 44 over  $j = 0, \dots, k-1$ , we can deduce  $2\sum_{j=1}^{k-1} [j\mathcal{G}(t^{j+1}, \mu^{j+1}) - j\mathcal{G}(t^j, \mu^j)]$  into Eq. 39, shown at the bottom of the next page.

Specifically, Eq. 39 show that the sequence of function value  $\{\mathcal{G}(t^k, \mu^k)\}$  converges to the optimal value  $\mathcal{G}(t^*, \mu^*)$  at a rate of convergence that is no worse than  $O(1/k)$ .

#### VI. PERFORMANCE EVALUATION

In this section, the proposed OTLT scheme is evaluated by comparing with other back-off control schemes. These schemes include: 1) a predefined back-off scheme in which the packet back-off duration in each transmission cycle is predefined as a constant value; 2) IEEE 802.15.4 MAC scheme in which the packet BSD is randomly selected from a uniform distribution. We use OMNET++ to evaluate the OTLT scheme. Specifically, we use the average packet sojourn time and deadline-miss ratio (DMR) to evaluate the performance of the proposed OTLT scheme. We define the DMR as the proportion of packets that do not arrive on time to the total number of packets [28]. The devices are uniformly deployed in a  $100 \times 100$ m area. The IIoT network is built on a star topology with all IIoT devices linked to a single central AP. The initial transmission power of each IIoT device is 0 dB. We evaluate and compare the proposed scheme to the two preceding schemes by changing the interference effects, the number of IIoT devices and the pre-defined packet transmission deadline.

As shown in Fig. 6, the channel model is defined as the sum of the power gains reflected from different scatterers in the industrial environment. Considering the properties of time-varying and multipath propagation, we express the channel model as  $h(t) = \sum_{m=0}^M \alpha_m(t) \cdot \delta(t - \tau_m(t)) \cdot e^{j(2\pi f_m t - \phi_m(t))} + J(t)$ , where  $\tau_m(t)$  is the delay caused by the  $m$ -th scatterer at time  $t$ ,  $\alpha_m$  is the power gain factor from the  $m$ -th scatterer,  $\phi_m(t)$  is the phase shift caused by the vibration of the  $m$ -th scatterer and  $f_m$  is the corresponding Doppler shift,  $J(t)$  is the summation of the noise and interference effects [15], [29]. We develop a two-state Markov model to simulate the noise and interference effects, which is defined as  $J(t) = b(t)J_g(t) + (1 - b(t))J_b(t)$ , where  $b(t)$  is a random variable with state space  $\{0, 1\}$ . Let  $J_g(t) = \sqrt{2}e^{j\omega t}$  be a good channel state in which the device can correctly detect the channel state. Let  $J_b(t) = \sum_{n=0}^N \sqrt{2}\beta_n e^{j\phi_n(t)} + n(t)$  be a bad channel state where the channel is distorted by interference signals from other wireless systems operating on the similar frequency band, where  $\sum_{n=0}^N \sqrt{2}\beta_n e^{j\phi_n(t)}$  is the summation of  $N$  interference signals,  $\beta_n$  is the  $n$ -th interference power,  $\phi_n(t)$  is the corresponding phase shift at time  $t$ ,  $n(t)$  is the noise following Gaussian distribution with zero mean. The transition probability of the two-state Markov process is  $p_{i,j} = P\{b(t+1) = i | b(t) = j\}$ , for  $i, j \in \{0, 1\}$ . Fig. 7 shows the channel fading process produced by the simulator, where the average fading duration of the channel fading induced by the impulse noise does not exceed 1 second. Fig. 7 also shows the results of the number of level crossing (LCN) per 0.1 second and the average duration of fading (AFD) per second. See [30] for details on the channel modelling. The details of simulation settings can be found in Table I. The path-loss exponent and shadowing variance parameters are obtained from real-life measurements in an industrial environments.

Fig. 8 shows the PDF of the packet sojourn time for different schemes. It can be seen that, in contrast to the determined time and random exponential scheme, the proposed OTLT scheme can successfully deliver most packets within 10 ms and confine the packet sojourn time to a specific time

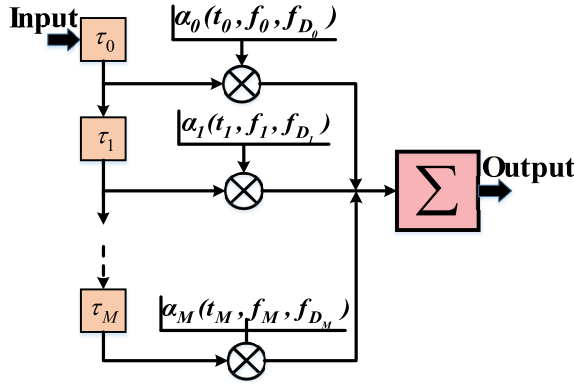


Fig. 6. Time-delay wireless channel model.

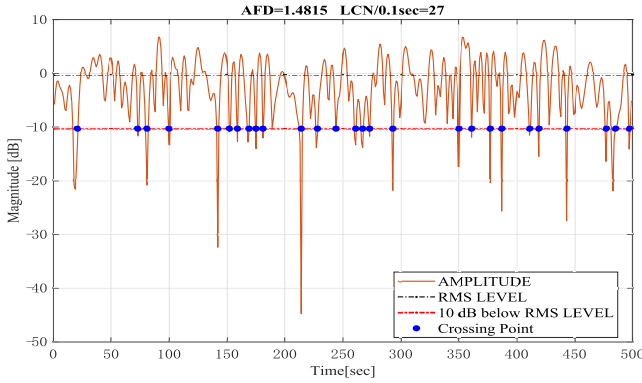


Fig. 7. Simulator Results labelled AFD and LCN.

boundary. This indicates that by managing the packet BSD in each transmission cycle and considering the corresponding maximum FPP, the distribution tail of the packet sojourn time can be controlled. In particular, the proposed TSM can combine each of the determined packet BSDs together in a way that characterize the entire feature of the packet sojourn time. Fig. 9 shows that the proposed OTLT scheme can reduce the packet sojourn time when compared to other schemes. Rather than acquiring a back-off duration in the other schemes, we attempt to minimize the objective function in order to obtain the optimal gradient and scale for controlling the packet

TABLE I  
SIMULATION SETTINGS

Wireless Channel Settings	
Name	Value
Frequency ( $f$ )	2.4 GHz
Simulation time ( $T$ )	300s
The number of scatters ( $M$ )	100
Transmit power ( $p_t$ )	Adaptive
Receiver noise figure ( $F$ )	11 dBm
Receiver noise bandwidth ( $B$ )	5 MHz
Noise temperature ( $T_n$ )	290 K
Transition probability from $J_g(t)$ to $J_b(t)$ ( $p_{01}$ )	0.005
Transition probability from $J_b(t)$ to $J_g(t)$ ( $p_{10}$ )	0.1
Number of interfering signals ( $N$ )	7
Total interference power ( $J$ )	4 dBm
Ricean K-factor of multipath component ( $K$ )	5 dBm
Relative permittivity of the reflecting surface at 2.4GHz ( $\eta$ )	$1 - j802$
Path-loss exponent ( $n$ )	1.72 [14]
Shadowing variation ( $\sigma$ )	3.76 [14]
Adaptor factor ( $\gamma$ )	0.2
Protocol Settings	
Name	Value
Devices payload size	28 Byte
MAC packet Overhead	14 Byte
Packet generation interval	$U(0.1, 5)$ ms
Superframe Order	61440 Symbols
Number of slot in a superframe	16
CCA mode	True
Back-off unit period	20 Symbols
Max SIFS frame size	18 Octets
Max BE_	5
Max Retry_	4
Min CAP length	440 Symbols

BSD while meeting the delay requirement. In addition, Fig. 9 shows that the OTLT scheme can also maintain the packet sojourn time within a stringent delay limitation. The reason is that, considering Eq. 19, the packet BSD is generated within the range of  $[0, \arg\max g_n(t)]$  to minimize the packet sojourn time while maximizing the transmission FPP. As a result, the proposed OTLT scheme can always meet the packet's latency stability criteria.

If the pre-configured packet deadline is gradually changed, as shown in Fig. 10, the OTLT scheme can still confine the packet sojourn time within the quantifiable delay limitation and variance requirements compared to other schemes. The number of devices, the probability to detect an interference

$$\begin{aligned}
2 \sum_{j=1}^{k-1} \left[ j \mathcal{G}(t^{j+1}, \mu^{j+1}) - j \mathcal{G}(t^j, \mu^j) \right] &\geq 2 \sum_{j=1}^{k-1} 2j \|(\mu^j - \mu^{j+1})\|^2 (\varepsilon^j)^{-1} \\
\Rightarrow 2 \left[ k \mathcal{G}(t^k, \mu^k) - \mathcal{G}(t^j, \mu^j) - \sum_{j=1}^{k-1} \mathcal{G}(t^{j+1}, \mu^{j+1}) \right] &\geq 2 \sum_{j=1}^{k-1} 2j \|(\mu^j - \mu^{j+1})\|^2 (\varepsilon^j)^{-1} \\
\Rightarrow 2k \left[ \mathcal{G}(t^k, \mu^k) - \mathcal{G}(t^*, \mu^*) \right] &\geq \|(\mu^k - \mu^*)\|^2 (\varepsilon^k)^{-1} - \|(\mu^0 - \mu^*)\|^2 (\varepsilon^0)^{-1} + \sum_{j=0}^{k-1} (2j+1) \|(\mu^j - \mu^{j+1})\|^2 (\varepsilon^j)^{-1} \\
\Rightarrow \mathcal{G}(t^*, \mu^*) - \mathcal{G}(t^k, \mu^k) &\leq \left( \|(\mu^0 - \mu^*)\|^2 (\varepsilon^0)^{-1} - \|(\mu^k - \mu^*)\|^2 (\varepsilon^k)^{-1} - \sum_{j=0}^{k-1} (2j+1) \|(\mu^j - \mu^{j+1})\|^2 (\varepsilon^j)^{-1} \right) / (2k) \\
\Rightarrow \mathcal{G}(t^*, \mu^*) - \mathcal{G}(t^k, \mu^k) &\leq \frac{\|(\mu^0 - \mu^*)\|^2 (\varepsilon^0)^{-1}}{2k}
\end{aligned} \tag{39}$$

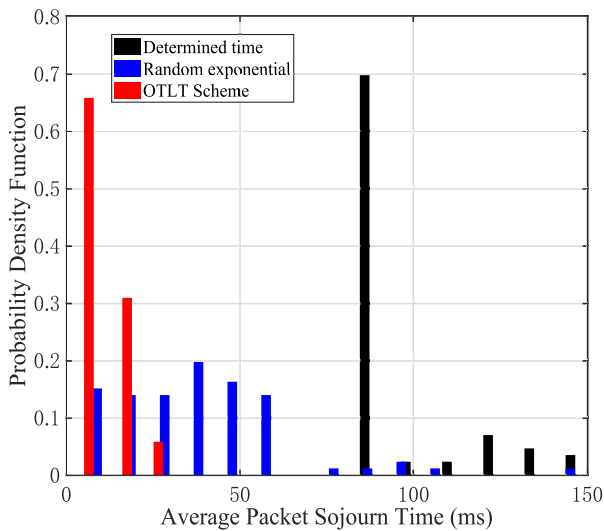


Fig. 8. PDF of packet sojourn time.

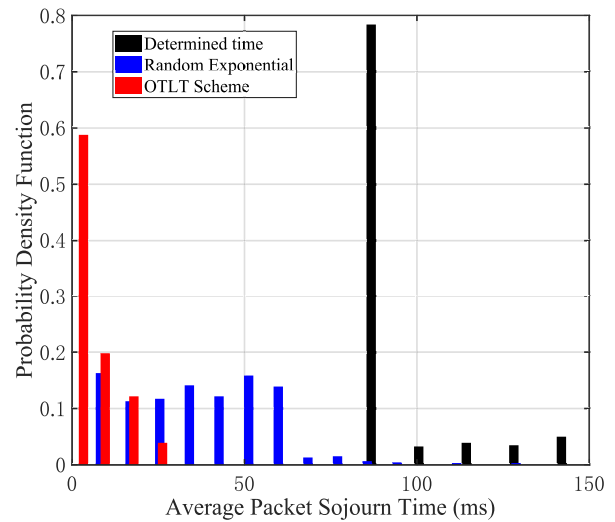


Fig. 10. PDF of packet sojourn time, deadline = 90 ms.

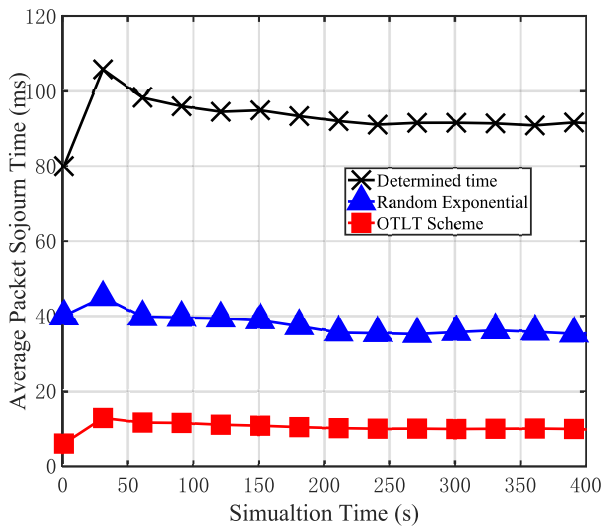


Fig. 9. Average packet sojourn time of different schemes.

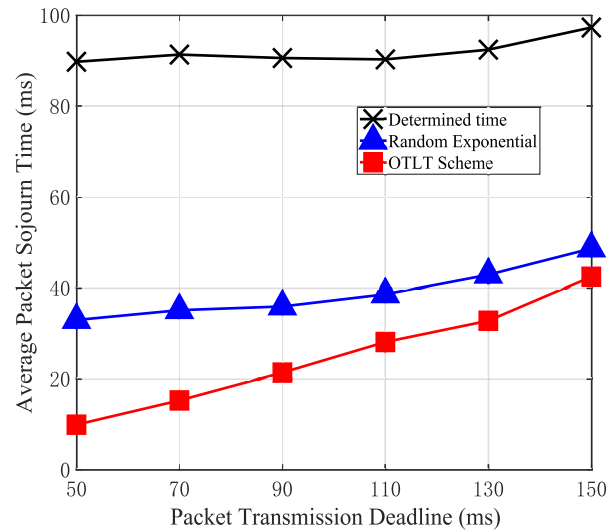


Fig. 11. Average packet sojourn time vs deadline.

and the pre-configured packet deadline in Fig. 10 are set as 10, 0.2 and 90 ms, respectively. The underlying reason is when the packet deadline is increased, the limitation of the total time constraint in Eq. 27 is also increased. Since the solution space is enlarged, it is necessary to generate the packet BSD along the control gradient of Eq. 27 in a larger control scale for the next transmission cycle. Fig. 11 shows the average packet sojourn time when the constraint of the packet transmission deadline is gradually increased. It can be seen that, when the deadline is extended, the average packet sojourn time of both the proposed OTLT scheme and the random exponential scheme increases, but the performance of the predefined back-off scheme does not change much. The reason is that the packet BSD derived from the OTLT scheme is calculated based on the quadratic barrier method with the deadline constraint. When the constraint space is expanded, the range of the available back-off result is also increased, which leads to an increase in the average packet sojourn time. When

the IIoT network employs the predefined back-off scheme, the time slot for each device to access the channel is assigned at the beginning of packet transmission. Thus, the average packet sojourn time with predefined back-off scheme remains unchanged when increasing the packet transmission deadline.

In Fig. 12, when the probability to detect a BUSY channel increases, the OTLT scheme performs better than other schemes in terms of latency. The reason is, at first, the OTLT scheme can detect the hidden channel state by the forward learning algorithm in Alg. 2. The learning method in the OTLT scheme can increase the detection accuracy. Then, according to the exact channel state and the corresponding access probability, the proposed TSM can generate a much proper value of the packet BSD through minimizing the packet sojourn time. Fig. 13 shows that the packet sojourn time increases as the number of devices increases. The busier the network becomes, the more collisions there will be, especially in an industrial environment. It also shows that the proposed

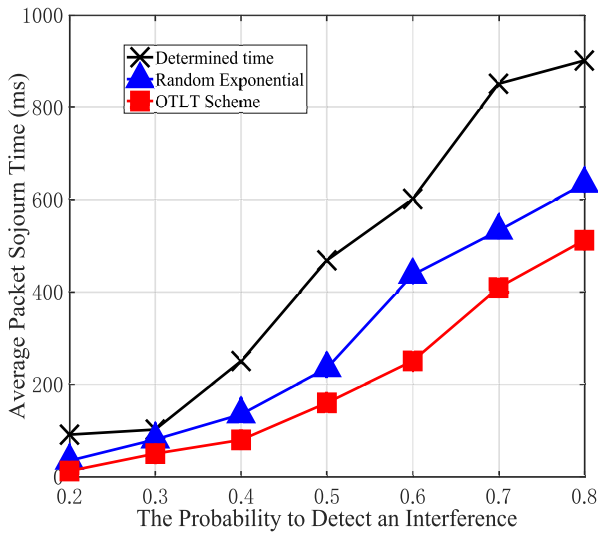


Fig. 12. Average packet sojourn time vs interference effect.

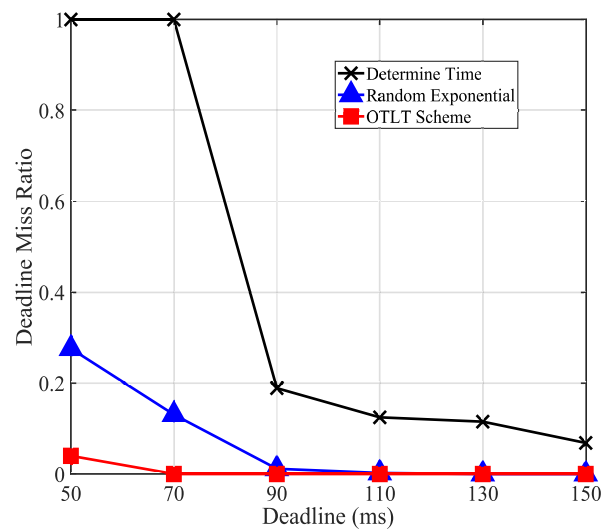


Fig. 14. DMR vs different deadline.

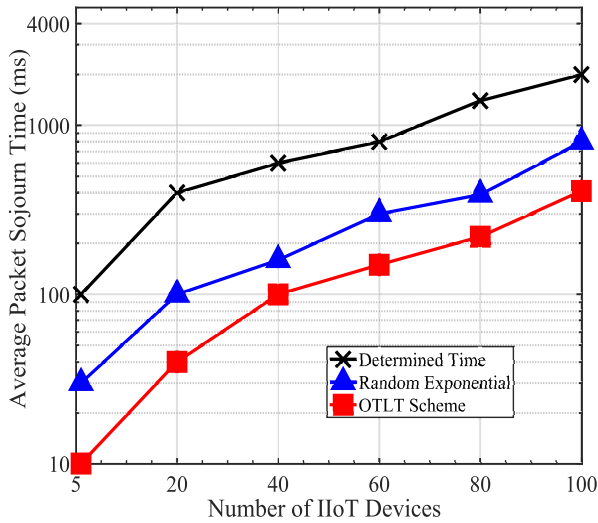


Fig. 13. Average packet sojourn time vs number of devices.

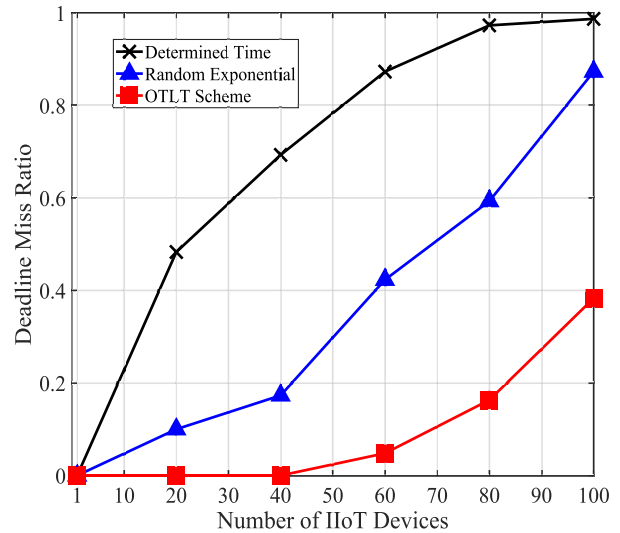


Fig. 15. DMR vs number of devices, deadline = 200ms.

OTLT scheme outperforms the other schemes. The reason is twofold. First, the fact that an IIoT device detects the channel as free and wants to transmit does not mean the channel is free around the receiver area. Through establishing the relation between the average duration and the transition probability among different hidden channel states, the OTLT scheme can proactively avoid the collision. Second, the OTLT scheme determines the packet sojourn time according to not only the limited latency constraints but also the maximum probability to successfully transmit the packet. Even when the device fails to access the channel, OTLT scheme can renew the objective function based on the preceding obtained packet BSD and search the new BSD results in the updated feasible region of the packet sojourn time by considering the penalty method.

As shown in Fig. 14, the DMR values of different schemes are compared in terms of the packet deadline. The DMR decreases with the increase in the pre-defined deadline. Compared with the benchmarks, the performance gain achieved by

the proposed OTLT scheme becomes obvious when shortening the deadline. Fig. 15 shows that the DMR increases with the increment of the devices. Two important observations can be drawn from the simulation results. First, when the number of devices is less than 40, the proposed OTLT scheme can 100% meet the packet transmission deadline. The random exponential schemes also present acceptable delay performance on meeting the deadline. Second, when the number of devices exceeds 40, the DMR of the conventional schemes increase significantly when compared to the OTLT scheme. One reason is that the OTLT scheme improves the successful channel access probability of IIoT devices. On the other hand, the deadline constraint of Eq. 20 is renewed in each transmission cycle, which refreshes the objective function in Eq. 40 and allows the OTLT scheme to keep track of the remaining time for packet transmission. As a result, regardless of the increasing number of devices, the OTLT scheme can always

generate the proper packet BSD to meet the transmission deadline.

## VII. CONCLUSION

In this paper, we have proposed a hidden channel learning-based latency taming scheme, called OTLT, in IIoT. In particular, we have developed an HSMM to increase the channel detection accuracy and proposed a TSM to characterize the distribution tail of the packet sojourn time so that the proper packet BSD can be generated in each transmission cycle while adhering to a pre-defined latency limitation. Simulation results have demonstrated that the distribution tail of the packet sojourn time can be tamed through investigating the average cumulative summation of all historical packet BSDs and the corresponding FPP. We expect this work can further promote research interests in tail taming of latency distribution, whose importance will be adamant in IIoT networks with the slew of unforeseen applications. Due to the stringent requirements of new industrial applications, the concepts of next-generation IIoT networks have shifted from reactive and centralized network towards proactive, large scale and fine-grained metrics like the delay distribution and probability bounds. Achieving one performance requirement is no longer an option but a necessity. Moreover, it becomes increasingly important to take into account several different requirements at the same time. For the future work, we are going to investigate the tradeoff between the network scale and the stringent latency distribution tail.

### APPENDIX A PROOF OF LEMMA 1

The sojourn time of each state follows a uniform distribution. Suppose  $f_{ij}(t)$  equals  $A$ , when  $t \in C$ ; and equals 0, otherwise. If  $C$  is a convex set,  $x, y \in C$ , and  $0 \leq t \leq 1$ , we have  $tx + (1-t)y \in C$ . Hence,  $f_{ij}(x) = f_{ij}(y) = f_{ij}[tx + (1-t)y] = A$ , which yields that  $f_{ij}[tx + (1-t)y] \geq tf_{ij}(x) + (1-t)f_{ij}(y)$ . When  $x$  or  $y$  is not in  $C$ , we have  $f_{ij}(x) = 0$  or  $f_{ij}(y) = 0$ , which also yields that  $f_{ij}[tx + (1-t)y] \geq tf_{ij}(x) + (1-t)f_{ij}(y)$ . Therefore, we can see that the sojourn time distribution in Fig. 3 follows concavity property. When  $n = 1$ ,  $w_{S_{lk}, S_{ji}} = p_{S_{lk}, S_{ji}} f_{S_{lk}, S_{ji}}(t)$ . Since  $p_{S_{lk}, S_{ji}}$  is a positive constant value and  $f_{S_{lk}, S_{ji}}(t)$  follows concavity property,  $w_{S_{lk}, S_{ji}}$  also follows concavity property. If  $f_{S_{lk}, S_{ji}}(t)$  and  $w_{S_{lk}, S_{ji}}$  is concave, the convolution,  $\int_0^t w_{S_{lk}, S_{ji}} f_{S_{lk}, S_{ji}}(t-\tau) d\tau$ , is also concave [31]. Since a nonnegative weighted sum of concave function is concave [31], after  $n$  iteration, we obtain that  $w_{S_{lk}, S_{ji}}$  keeps its concavity property. As shown in Eq. 17, it can be easily seen that, the subset of  $w_{S_{lk}, S_{ji}}$ ,  $g_{S_{lk}, S_{ji}}(t)$  also follows a concave property.

### APPENDIX B PROOF OF LEMMA 2

We use a quadratic penalty term to prevent feasible iterates from moving too close to the limitation of packet BSD in each device. A constant,  $\varepsilon$ , is multiplied by the suggested quadratic penalty function to determine the penalty severity for breaching the constraint. Then, we add the quadratic penalty

term to the Lagrangian function of the objective function. The sequence of objective function outcomes generated by the multiplier method converges to the optimum result at a linear rate proportional to the number of iterations. It implies that the multiplier method can significantly reduce the computation time. Convert Eq. 20 to equality constrained problem

$$\begin{aligned} & \operatorname{argmin}_t \sum_{i=1}^n (1 - g_i(t) + B_i t_i g_i(t_i) + (n-i)A_i) \\ & + \frac{\varepsilon}{2} \left\| \sum_{i=1}^n t_i - T + z^2 \right\|^2 \\ \text{s.t. } & B_i = \prod_{j=1}^{i-1} \hat{g}_j(t_j), \quad A_i = \prod_{j=1}^i \hat{g}_j(t_j) \\ & t_{i \in \{1, \dots, n\}} \in \operatorname{argmax}_t g_{i \in \{1, \dots, n\}}(t), \\ & \sum_{i=1}^n t_i - T + z^2 = 0 \end{aligned} \quad (40)$$

where  $z$  is additional variable. We use  $u$  instead of  $z^2$  and minimize the unconstrained minimizations of Eq. 40 with respect to  $z$  as

$$\begin{aligned} \bar{\mathcal{J}}(\mathbf{t}, \mu) &= \min_u \mathcal{J}(\mathbf{t}, u, \mu) \\ &= \sum_{i=1}^n (1 - g_i(t) + B_i t_i g_i(t_i) + (n-i)A_i) \\ & + \min_{u \geq 0} \left\{ \mu \left[ \sum_{i=1}^n t_i - T + u \right] \right. \\ & \left. + \frac{\varepsilon}{2} \left\| \sum_{i=1}^n t_i - T + u \right\|^2 \right\} \end{aligned} \quad (41)$$

The constrained minimum of Eq. 41 is  $u^* = \max\{0, \hat{u}\}$ , where  $\hat{u}$  is the unconstrained minimum with the derivative of 0.

$$\begin{aligned} 0 &= \nabla_u \mathcal{J}(\mathbf{t}, u, \mu) = \mu + \varepsilon \left( \sum_{i=1}^n t_i - T + u \right) \\ \Rightarrow \hat{u} &= -\frac{\mu}{\varepsilon} - \left( \sum_{i=1}^n t_i - T \right) \end{aligned} \quad (42)$$

Thus, we have

$$\begin{aligned} u^* &= \max\left\{0, -\frac{\mu}{\varepsilon} - \left( \sum_{i=1}^n t_i - T \right)\right\} \\ \Leftrightarrow -\frac{\mu}{\varepsilon} - \left( \sum_{i=1}^n t_i - T \right) + u^* &= \max\left\{\sum_{i=1}^n t_i - T, -\frac{\mu}{\varepsilon}\right\} \end{aligned} \quad (43)$$

Substituting (43) into (41), we obtain

$$\begin{aligned} \bar{\mathcal{J}}(\mathbf{t}, \mu) &= \sum_{i=1}^n (1 - g_i(t) + B_i t_i g_i(t_i) + (n-i)A_i) \\ & + \frac{1}{2\varepsilon} \left\{ \left[ \max\left(\varepsilon \left( \sum_{i=1}^n t_i - T \right) + \mu, 0\right) \right]^2 - \mu^2 \right\} \end{aligned} \quad (44)$$

Taking derivatives of Eq. 44 with respect to  $\mu$ , the Lagrange multiplier  $\mu^*$  can be updated as

$$\mu^{k+1} = \mu^k + \max\left(\varepsilon^k \left(\sum_{i=1}^n t_i - T\right), -\mu^k\right) \quad (45)$$

Thus, if  $\varepsilon^k$  is less than  $(1 - B_i t_i) \nabla_{t_i t_i}^2 g_i(t_i) - 2B_i \nabla_{t_i} g_i(t_i)$  in accordance with  $\nabla_{t_i t_i}^2 \bar{J}(\mathbf{t}, \mu) > 0$ , the penalty function can force the BSD to remain away from the latency boundary and can be expressed as

$$\frac{1}{2\varepsilon} \left[ \max\left(\varepsilon \left(\sum_{i=1}^n t_i - T\right) + \mu, 0\right) \right]^2 - \frac{1}{2\varepsilon} \mu^2 \quad (46)$$

From Eq. 46, if the summation of all past BSD of the packet  $\sum_{i=1}^n t_i$  is smaller than  $T - \frac{\mu}{\varepsilon}$ , no extra punishment is provided. In each transmission cycle,  $t_i$  should be initialized based on the value of  $T - \frac{\mu}{\varepsilon}$ . When  $\sum_{i=1}^n t_i$  is larger than  $T$ , Eq. 46 gives a large punishment to Eq. 44 with iteratively difference between  $\sum_{i=1}^n t_i$  and  $T$ .

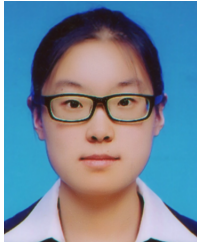
## REFERENCES

- [1] X. Shen et al., "AI-assisted network-slicing based next-generation wireless networks," *IEEE Open J. Veh. Technol.*, vol. 1, pp. 45–66, 2020.
- [2] S. Hu and W. Chen, "Joint lossy compression and power allocation in low latency wireless communications for IIoT: A cross-layer approach," *IEEE Trans. Commun.*, vol. 69, no. 8, pp. 5106–5120, Aug. 2021.
- [3] D. Yu, W. Li, H. Xu, and L. Zhang, "Low reliable and low latency communications for mission critical distributed industrial Internet of Things," *IEEE Commun. Lett.*, vol. 25, no. 1, pp. 313–317, Jan. 2020.
- [4] W. Wu, P. Yang, W. Zhang, C. Zhou, and X. Shen, "Accuracy-guaranteed collaborative DNN inference in industrial IoT via deep reinforcement learning," *IEEE Trans. Ind. Informat.*, vol. 17, no. 7, pp. 4988–4998, Jul. 2021.
- [5] M. Li, C. Chen, H. Wu, X. Guan, and X. Shen, "Age-of-information aware scheduling for edge-assisted industrial wireless networks," *IEEE Trans. Ind. Informat.*, vol. 17, no. 8, pp. 5562–5571, Aug. 2020.
- [6] L. Liu and W. Yu, "A D2D-based protocol for ultra-reliable wireless communications for industrial automation," *IEEE Trans. Wireless Commun.*, vol. 17, no. 8, pp. 5045–5058, Aug. 2018.
- [7] M. Raza, N. Aslam, H. Le-Minh, S. Hussain, Y. Cao, and N. M. Khan, "A critical analysis of research potential, challenges, and future directives in industrial wireless sensor networks," *IEEE Commun. Surveys Tuts.*, vol. 20, no. 1, pp. 39–95, 1st Quart., 2018.
- [8] M. K. Abdel-Aziz, S. Samarakoon, C.-F. Liu, M. Bennis, and W. Saad, "Optimized age of information tail for ultra-reliable low-latency communications in vehicular networks," *IEEE Trans. Commun.*, vol. 68, no. 3, pp. 1911–1924, Mar. 2019.
- [9] E. Asyabi, S. SanaeeKohroudi, M. Sharifi, and A. Bestavros, "TerrierTail: Mitigating tail latency of cloud virtual machines," *IEEE Trans. Parallel Distrib. Syst.*, vol. 29, no. 10, pp. 2346–2359, Oct. 2018.
- [10] S. R. Khosravirad, H. Viswanathan, and W. Yu, "Exploiting diversity for ultra-reliable and low-latency wireless control," *IEEE Trans. Wireless Commun.*, vol. 20, no. 1, pp. 316–331, Jan. 2021.
- [11] Q. Li, K. Zhang, M. Cheffena, and X. Shen, "Channel-based sampling rate and queuing state control in delay-constrained industrial WSNs," in *Proc. IEEE Global Commun. Conf. (GLOBECOM)*, Dec. 2017, pp. 1–6.
- [12] Y. Cui, V. K. N. Lau, R. Wang, H. Huang, and S. Zhang, "A survey on delay-aware resource control for wireless systems—Large deviation theory, stochastic Lyapunov drift, and distributed stochastic learning," *IEEE Trans. Inf. Theory*, vol. 58, no. 3, pp. 1677–1701, Mar. 2012.
- [13] M. Bennis, M. Debbah, and H. V. Poor, "Ultrareliable and low-latency wireless communication: Tail, risk, and scale," in *Proc. IEEE*, vol. 106, no. 10, pp. 1834–1853, Oct. 2018.
- [14] Y. Ai, M. Cheffena, and Q. Li, "Radio frequency measurements and capacity analysis for industrial indoor environments," in *Proc. 9th Eur. Conf. Antennas Propag. (EuCAP)*, Apr. 2015, pp. 1–5.
- [15] C. Cano, G. H. Sim, A. Asadi, and X. Vilajosana, "A channel measurement campaign for mmWave communication in industrial settings," *IEEE Trans. Wireless Commun.*, vol. 20, no. 1, pp. 299–315, Jan. 2020.
- [16] J. W. Cho and Y. Jiang, "Fundamentals of the backoff process in 802.11: Dichotomy of the aggregation," *IEEE Trans. Inf. Theory*, vol. 61, no. 4, pp. 1687–1701, Apr. 2015.
- [17] *IEEE Standard for Local and Metropolitan Area Networks—Part 15.4: Low-Rate Wireless Personal Area Networks (LR-WPANs)*, Standard 802.15.4-2011, 2011.
- [18] N. H. Mahmood et al., "White paper on critical and massive machine type communication towards 6G," 2020, *arXiv:2004.14146*.
- [19] A. Ghosh, A. Maeder, M. Baker, and D. Chandramouli, "5G evolution: A view on 5G cellular technology beyond 3GPP release 15," *IEEE Access*, vol. 7, pp. 127639–127651, 2019.
- [20] D. H. Wilkinson, "Ionization energy loss by charged particles part I. The Landau distribution," *Nucl. Instrum. Methods Phys. Res. A, Accel. Spectrom. Detect. Assoc. Equip.*, vol. 383, nos. 2–3, pp. 513–515, Dec. 1996.
- [21] A. Bhowmick, K. Yadav, and S. D. Roy, "Throughput of an energy harvesting cognitive radio network based on prediction of primary user," *IEEE Trans. Veh. Technol.*, vol. 66, no. 9, pp. 8119–8128, Sep. 2017.
- [22] H. Eltom, S. Kandeepan, Y. C. Liang, B. Moran, and R. J. Evans, "HMM based cooperative spectrum occupancy prediction using hard fusion," in *Proc. IEEE Int. Conf. Commun. (ICC)*, May 2016, pp. 669–675.
- [23] L. Sanabria-Russo, J. Barcelo, B. Bellalta, and F. Gringoli, "A high efficiency MAC protocol for WLANs: Providing fairness in dense scenarios," *IEEE/ACM Trans. Netw.*, vol. 25, no. 1, pp. 492–505, Feb. 2016.
- [24] J. D. Kim, D. I. Laurenson, and J. S. Thompson, "Centralized random backoff for collision resolution in Wi-Fi networks," *IEEE Trans. Wireless Commun.*, vol. 16, no. 9, pp. 5838–5852, Sep. 2017.
- [25] R. D. Gomes, C. Benavente-Peces, I. E. Fonseca, and M. S. Alencar, "Adaptive and beacon-based multi-channel protocol for industrial wireless sensor networks," *J. Netw. Comput. Appl.*, vol. 132, pp. 22–39, Apr. 2019.
- [26] C.-F. Liu and M. Bennis, "Taming the tail of maximal information age in wireless industrial networks," *IEEE Commun. Lett.*, vol. 23, no. 12, pp. 2442–2446, Dec. 2019.
- [27] Q. Liu, S. Xu, C. Lu, H. Yao, and H. Chen, "Early recognition of driving intention for lane change based on recurrent hidden semi-Markov model," *IEEE Trans. Veh. Technol.*, vol. 69, no. 10, pp. 10545–10557, Oct. 2020.
- [28] Q. Li, N. Zhang, M. Cheffena, and X. Shen, "Channel-based optimal back-off delay control in delay-constrained industrial WSNs," *IEEE Trans. Wireless Commun.*, vol. 19, no. 1, pp. 696–711, Jan. 2020.
- [29] Q. Li, K. Zhang, M. Cheffena, and X. Shen, "Exploiting dispersive power gain and delay spread for Sybil detection in industrial WSNs," in *Proc. IEEE/CIC ICC*, Jul. 2016, pp. 1–6.
- [30] M. Cheffena, "Industrial wireless sensor networks: Channel modeling and performance evaluation," *EURASIP J. Wireless Commun. Netw.*, vol. 2012, no. 1, pp. 1–8, Sep. 2012.
- [31] S. Boyd and L. Vandenberghe, *Convex Optimization*. Cambridge, U.K.: Cambridge Univ. Press, 2003.



**Qihao Li** (Member, IEEE) received the M.Sc. degree in information and communication technology from the University of Agder, Norway, in 2013, and the Ph.D. degree from the Department of Electrical and Computer Engineering, University of Oslo, Norway, in 2019. In 2019, he was a Visiting Researcher at the Department of Electrical and Computer Engineering, University of Waterloo, Waterloo, ON, Canada. In 2020, he was a Post-Doctoral Fellow with the Department of Electrical and Computer Engineering, University of Waterloo. He is currently

a Lecturer with the School of Electrical Engineering and Intelligentization, Dongguan University of Technology, China. His current research focuses on industrial wireless sensor networks, optimal control and optimization, wireless network security, and localization. He served as a member of the Technical Program Committee for IEEE GLOBECOM 2019–2022, IEEE ICC 2019–2022, IEEE CIC ICC 2017–2022, EuCAP 2019, and BDEC-SmartCity 2018.



**Jiayin Chen** (Member, IEEE) received the B.E. and M.S. degrees from the School of Electronics and Information Engineering, Harbin Institute of Technology, Harbin, China, in 2014 and 2016, respectively, and the Ph.D. degree from the Department of Electrical and Computer Engineering, University of Waterloo, Waterloo, ON, Canada, in 2021. Since 2021, she has been a Post-Doctoral Fellow with the Department of Electrical and Computer Engineering, The University of British Columbia, Vancouver, BC, Canada. Her research interests are in the area of

vehicular networks, machine learning, and self-organized networks, with current focus on sidelink communication technology-based self-organized networks.



**Michael Cheffena** received the M.Sc. degree in electronics and computer technology from the University of Oslo, Norway, in 2005, and the Ph.D. degree from the Norwegian University of Science and Technology (NTNU), Gjøvik, Trondheim, in 2008. In 2007, he was a Visiting Researcher at the Communications Research Center, Canada. From 2009 to 2010, he conducted a post-doctoral study at the University Graduate Center, Kjeller, Norway, and the French Space Agency, Toulouse. He is currently a Full Professor at NTNU. His

research interests include modeling and prediction of propagation radio channels, signal processing, and medium access control (MAC) protocol design.



**Xuemin (Sherman) Shen** (Fellow, IEEE) received the Ph.D. degree in electrical engineering from Rutgers University, New Brunswick, NJ, USA, in 1990. He is currently a University Professor with the Department of Electrical and Computer Engineering, University of Waterloo, Waterloo, ON, Canada. His research focuses on resource management in interconnected wireless/wired networks, wireless network security, social networks, smart grid, and vehicular ad hoc and sensor networks. He is a Registered Professional Engineer of Ontario, Canada; a

fellow of the Engineering Institute of Canada, the Canadian Academy of Engineering, and the Royal Society of Canada; and a Foreign Member of the Chinese Academy of Engineering. He was a recipient of the Canadian Award for Telecommunications Research from the Canadian Society of Information Theory (CSIT) in 2021, the R. A. Fessenden Award in 2019 from IEEE, Canada, the Award of Merit from the Federation of Chinese Canadian Professionals (Ontario) in 2019, the James Evans Avant Garde Award in 2018 from the IEEE Vehicular Technology Society, the Joseph LoCicero Award in 2015 and Education Award in 2017 from the IEEE Communications Society, and the Technical Recognition Award from the Wireless Communications Technical Committee (2019) and AHSN Technical Committee (2013). He was also a recipient of the Excellent Graduate Supervision Award in 2006 from the University of Waterloo and the Premier's Research Excellence Award (PREA) in 2003 from the Province of Ontario, Canada. He was the Technical Program Committee Chair/the Co-Chair of IEEE GLOBECOM 2016, IEEE Infocom 2014, IEEE VTC 2010 Fall, and IEEE GLOBECOM 2007, and the Chair of IEEE Communications Society Technical Committee on Wireless Communications. He is the President of IEEE Communications Society. He was the Vice President of technical and educational activities, the Vice President for Publications, a Member-at-Large on the Board of Governors, the Chair of the Distinguished Lecturer Selection Committee, and a member of the IEEE Fellow Selection Committee of the ComSoc. He was the Editor-in-Chief of the IEEE INTERNET OF THINGS JOURNAL, *IEEE Network*, and *IET Communications*. He is the Distinguished Lecturer of IEEE Vehicular Technology Society and IEEE Communications Society.